AD-A133 747 AMPLIFICATION OF SOUND BY GAS PHASE REACTIONS(U) 1/2
MISSISSIPPI UNIV UNIVERSITY PHYSICAL ACOUSTICS RESEARCH
GROUP H E BASS ET AL. 11 OCT 83 PARGUM-83-02
UNCLASSIFIED N00014-81-K-0691 F/G 7/4 NL

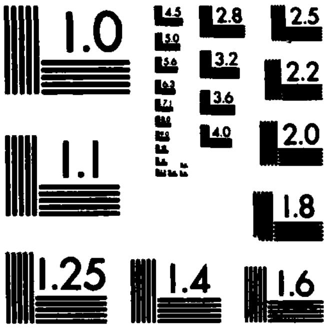

MICROCOPY RESOLUTION TEST CHART
NATIONAL BUREAU OF STANDARDS-1963-A

(12)

Amplification of Sound by
Gas Phase Reactions

PARGUM Report 83-02

THE UNIVERSITY OF MISSISSIPPI
PHYSICAL ACOUSTICS RESEARCH GROUP
DEPARTMENT OF PHYSICS AND ASTRONOMY

Interim Technical Report

for

Office of Naval Research

Contract N00014-81-K-0691

Amplification of Sound by Gas Phase Reactions

PARGUM Report 83-02

by

Henry E. Bass and Richard M. Detsch
Physical Acoustics Research Laboratory
Department of Physics and Astronomy
The University of Mississippi
University, Mississippi 38677

October 11, 1983

Unclassified
SECURITY CLASSIFICATION OF THIS PAGE *(When Data Entered)*

REPORT DOCUMENTATION PAGE	READ INSTRUCTIONS BEFORE COMPLETING FORM
1. REPORT NUMBER PARGUM-83-02 ✓ — 2. GOVT ACCESSION NO. AD-A133 947	3. RECIPIENT'S CATALOG NUMBER
4. TITLE *(and Subtitle)* Amplification of Sound by Gas Phase Reactions	5. TYPE OF REPORT & PERIOD COVERED Interim Technical 6. PERFORMING ORG. REPORT NUMBER
7. AUTHOR(s) Henry E. Bass and Richard M. Detsch	8. CONTRACT OR GRANT NUMBER(s) N00014-81-K-0691
9. PERFORMING ORGANIZATION NAME AND ADDRESS Physical Acoustics Research Laboratory Department of Physics and Astronomy The University of Mississippi, Univ., MS 38677	10. PROGRAM ELEMENT, PROJECT, TASK AREA & WORK UNIT NUMBERS NR 384-836
11. CONTROLLING OFFICE NAME AND ADDRESS Office of Naval Research, Physics Division Code 412, Arlington, VA 22217	12. REPORT DATE 11 Oct. 83 13. NUMBER OF PAGES
14. MONITORING AGENCY NAME & ADDRESS *(if different from Controlling Office)*	15. SECURITY CLASS. *(of this report)* Unclassified 15a. DECLASSIFICATION/DOWNGRADING SCHEDULE

16. DISTRIBUTION STATEMENT *(of this Report)*

Approved for public release; distribution unlimited

17. DISTRIBUTION STATEMENT *(of the abstract entered in Block 20, if different from Report)*

18. SUPPLEMENTARY NOTES

19. KEY WORDS *(Continue on reverse side if necessary and identify by block number)*

Sound amplification
Chemical relaxation
Vibrational relaxation

20. ABSTRACT *(Continue on reverse side if necessary and identify by block number)*

A four year study of sound propagation in chemically reacting mixtures has led to experimental observation of sound amplification. Photo-initiated Cl_2-H_2-inert gas reactions provided the energy for the amplification observed. Amplification experiments were conducted in two modes which we termed pulsed and cw. For the pulsed experiments, high intensity UV-flash lamps dissociated molecular chlorine at the start of the experiments and the Cl_2-H_2-Ar reactions quickly went to completion; amplification was observed for about

cont

DD FORM 1 JAN 73 1473 EDITION OF 1 NOV 65 IS OBSOLETE
S/N 0102-LF-014-6601

Unclassified
SECURITY CLASSIFICATION OF THIS PAGE *(When Data Entered)*

cont 6 msec. The measured gain was 1.8 at 2 kHz compared to a gain of 4 predicted by theory. The source of this difference has not been resolved completely.

In cw experiments, low intensity UV-fluorescent lamps dissociated molecular chlorine continuously during the experiments, this extended the time over which amplification was observed to about 800 msec. Experiments were conducted for three Cl_2-H_2-SF_6 mixtures and four frequencies, 1.0, 2.5, 4.0, and 6.5 kHz. Computer calculations correctly predicted the frequency dependence of amplification and gave amplification values which were in fair agreement with observation.

Attenuation measurements were conducted for several Cl_2-SF_6 and H_2-SF_6 mixtures. These data were used to calculate vibrational relaxation times for SF_6 in collisions with Cl_2, H_2, and SF_6 molecules. The vibrational relaxation times were used to predict vibrational relaxation attenuation in Cl_2-H_2-SF_6 mixtures used in cw amplification experiments.

Foreword

This report is an adaptation of Richard Mark Detsch's Ph.D. dissertation "Amplification of Sound by Gas Phase Reactions" which was accepted by the faculty of the Department of Physics and Astronomy at the University of Mississippi on September 26, 1983. The work reported was carried out at the University of Mississippi's Physical Acoustics Research Laboratory with support from The National Science Foundation and the Office of Naval Research.

Henry E. Bass
Dissertation Director

ABSTRACT

AMPLIFICATION OF SOUND BY GAS-PHASE REACTIONS

DETSCH, RICHARD MARK. B.S., Pennsylvania State University, 1977. M.S., Western Kentucky University, 1979. Ph.D., University of Mississippi, 1983. Dissertation directed by Professor Henry E. Bass.

A four year study of sound propagation in chemically reacting mixtures has led to experimental observation of sound amplification. Photo-initiated Cl_2-H_2-inert gas reactions provided the energy for the amplification observed. Amplification experiments were conducted in two modes which we termed pulsed and cw. For the pulsed experiments, high intensity UV-flash lamps dissociated molecular chlorine at the start of the experiments and the Cl_2-H_2-Ar reactions quickly went to completion; amplification was observed for about 6 msec. The measured gain was 1.8 at 2 kHz compared to a gain of 4 predicted by theory. The source of this difference has not been resolved completely.

In cw experiments, low intensity UV-fluorescent lamps dissociated molecular chlorine continuously during the experiments, this extended the time over which amplification was observed to about 800 msec. Experiments were conducted for three Cl_2-H_2-SF_6 mixtures and four frequencies, 1.0, 2.5, 4.0, and 6.5 kHz. Computer calculations correctly predicted the frequency dependence of amplification and gave amplification values which were in fair agreement with observation.

Attenuation measurements were conducted for several Cl_2-SF_6 and H_2-SF_6 mixtures. These data were used to calculate vibrational relaxation times for SF_6 in collisions with Cl_2, H_2, and SF_6 molecules. The vibrational relaxation times were used to predict vibrational relaxation attenuation in Cl_2-H_2-SF_6 mixtures used in cw amplification experiments.

TABLE OF CONTENTS

LIST OF TABLES v

LIST OF FIGURES vi

Chapter

I. INTRODUCTION 1

II. THEORY 4

Introduction 4

General Formalism for Non-Equilibrium Thermodynamics 6

Attenuation 15

Reaction Details 19

III. APPARATUS 21

IV. EXPERIMENTAL RESULTS 37

Pulsed SACER 37

cw-SACER 46

Attenuation Measurements 57

V. CONCLUSIONS AND SUMMARY 67

REFERENCES 70

APPENDIX A. COMPUTER PROGRAMS USED TO PREDICT AMPLIFICATION 72

APPENDIX B. ELECTRONIC EQUIPMENT BUILT IN OUR LAB FOR cw SYSTEM . . . 88

BIOGRAPHICAL SKETCH OF THE AUTHOR 93

LIST OF TABLES

Table Page

I. Equipment List 26

II. Pulsed SACER Results 39

III. cw-SACER Data 50

IV. cw-SACER Data Comparison 53

V. Time Dependence of cw-SACER Amplification 55

VI. Attenuation Experiment # A1 Gas Mixture 100% SF_6 60

VII. Attenuation Experiment # AT3 Gas Mixture 20% Cl_2/80% SF_6 . . 61

VIII. Attenuation Experiment # AT6 Gas Mixture 50% Cl_2/50% SF_6 . . 62

IX. Attenuation Experiment # AT4 Gas Mixture 10% H_2/90% SF_6. . . 63

X. Attenuation Experiment # AT5 Gas Mixture 20% H_2/80% SF_6. . . 64

XI. Vibrational Relaxation Values For SF_6, SF_6-H_2, and SF_6-Cl_2 . 65

LIST OF FIGURES

Figure Page

1. cw System 22

2. Pulsed Sacer 23

3. Transducer for cw System 25

4. Reduced Area High Voltage Plate 28

5. Electronics for Transducers in cw System 29

6. Electronics for UV-Lamps Used with cw-SACER 31

7. Electronics for UV-Flash Lamps Used in Pulsed System 32

8. Minicomputer System Used to Control cw-SACER 33

9. Unfiltered Output from Pulsed SACER Experiment Cl_2-4.6 Torr; H_2=0.7 Torr; Ar-4.2 Torr 41

10. Signal Strength Versus Propagation Distance for 2kHz Signal . 43

11. Signal Strength Versus Propagation Distance for 2kHz Signal . 44

12. Cl_2 Pressure Versus Pressure Pulse 250 Joules Two Flash Lamps 47

13. Pressure Amplitude Versus Propagation Distance 49

14. $\Delta\alpha$ Versus Frequency for cw-SACER Experiments 51

15. $\Delta\alpha$ Versus Time for cw-SACER Experiments 56

16. Pressure Amplitude Versus Propagation Distance for Attenuation Experiment 58

CHAPTER 1

INTRODUCTION

The interaction between nonequilibrium chemical reactions and sound waves propagating in the reacting mixture affect a variety of observable phenomena, e.g. combustion instability in jet and rocket engines, structure of detonation waves, and turbulence in reacting flows. Studies which isolate the effects of the interaction are quite limited. There is reason to believe[1] that this interaction might lead to several new phenomena or explanations of unexplained observations. Among these are acoustic stimulation of chemical oscillations and chemical instability, amplification of sound, changes in sound speed and frequency during the course of the reaction, and sound induced changes in reaction rates. In this dissertation, amplification of sound will be of primary interest. While some phenomena may be observable at near equilibrium conditions[2-4], extreme nonequilibrium conditions are required for measurable sound amplification[1]. There have been a number of theoretical studies of sound amplification in irreversibly reacting mediums[5-13]. Experimental verification of this phenomenon, however, is limited[6]. Related mechanisms for producing sound amplification in a gas include ionization of a gas[14], pressure dependence of infrared absorption[15], and selective excitation of internal modes[16]. Experimental verification of these mechanisms is also limited.

Devices which amplify sound directly will be refered to in the following as SACERS (<u>S</u>ound <u>A</u>mplification by <u>C</u>ontrolled <u>E</u>xcitation <u>R</u>eactions).

The purpose of this investigation was to observe sound amplification in a chemically reacting gas mixture (a chemical SACER). The H_2-Cl_2-buffer gas photoinduced chemical reaction was chosen for several reasons: the gases could be mixed without reacting and then UV-irradiated to initiate the reactions at a controlled time; most of the reaction rates, activation energies, etc. were known; and several theoretical studies had been done on this reaction scheme[5-8]. Acoustic frequencies in the range of 1-10kHz were chosen because lower frequencies, having periods longer than the relaxation times of the reactions, introduce theoretical complications; absorption calculations in this range have been done previously in this lab; and higher frequencies have increased attenuation making it more difficult to observe amplification.

Two SACERs were constructed for this investigation. The first consisted of a Cl_2-H_2-Ar gas filled tube surrounded by high intensity flash lamps. The tube was transparent to UV-radiation except for small unilluminated regions at each end. The flash lamps completely dissociated Cl_2 in the illuminated region causing a pressure increase which expanded into the unilluminated regions. This expansion led to pulses which propagated down the tube. A microphone recorded the amplitude of these pulses at various propagation distances. Electronic filters were used to study individual frequencies found in the pulses. This SACER is described as operating in a pulsed mode because, after flashing, the reactions lasted only about 10 msec (the time required to use all the H_2).

The second SACER used low intensity flourescent lamps to dissociate Cl_2. Since only a small amount of Cl_2 was dissociated at any given time, the reactions continued much longer (approx. 1 sec); we refer to this as the cw-SACER (continuous wave). Another reason for the slower reaction rate was the substitution of SF_6 for Ar. SF_6 has a larger specific heat which slowed the temperature increase of the gas. By keeping the translational temperature low the reactions evolved less rapidly. In this system there were no unilluminated regions; tone bursts were generated by a sending transducer. A receiving transducer measured the amplitude of the tone burst after propagating various distances through the reacting gas.

A necessary part of this study was measurement of sound attenuation in various SF_6-Cl_2 and SF_6-H_2 mixtures. From these measurements vibrational relaxation times of SF_6 could be predicted for the Cl_2-H_2-SF_6 mixtures which made it possible to calculate the attenuation due to vibrational relaxation in cw-SACER experiments.

Chapter II presents a mathematical and physical description of sound amplification in chemically reacting systems. Also described is the theory of sound attenuation, including that due to vibrational relaxation. The theory is not original to this work and is presented only for the benefit of the reader unfamiliar with previous work in the field. This study did require that the gain calculation of Gilbert[5,6] be meshed with the attenuation calculations based on work by Shields[17]. That step will be described in more detail. The primary thrust of this study was collection and analysis of experimental data. Most effort was expended in construction of the experimental apparatus described in Chapter III. Chapter III includes a description of the acoustic waveguides, the UV-radiation sources, and the computer system which controlled the cw-SACER. Chapter IV gives experimental results. Conclusions are discussed in Chapter V.

CHAPTER II

THEORY

Introduction

Two conditions can generate sound amplification in gas-phase, chemically reacting systems. The first occurs when the reaction has an imbalance of stoichiometric coefficients and a pressure dependent reaction rate. Sound modulates the pressure causing spacial fluctuations in the reaction rate. The rate fluctuations are accompanied by fluctuations in total atom concentration and hence secondary pressure fluctuations. As an example consider the reaction

$$A \xrightarrow{R} B + C \qquad (1)$$

where the reaction rate, R(p) increases monotonically with pressure. As the reaction progresses, the overall pressure is increasing, however, the rate of pressure increase is modulated by the acoustic signal. The reaction rate is larger in compressed regions causing a relative increase in pressure due to the imbalance of stoichiometric coefficients. The increase in pressure caused by the sound results in a feedback mechanism yielding a further increase in pressure. A similar feedback mechanism occurs in rarefied regions thus the acoustic signal is amplified. Reversing the pressure dependence of the reaction rate or the stoichiometric imbalance results in negative feedback.

The second amplification mechanism occurs when the reaction is exothermic and has a reaction rate that increases with temperature. Under adiabatic conditions, sound modulates the temperature and thus the reaction rate. In regions of positive temperature change, reaction rate and heat generation are increased causing a secondary temperature increase. Reversing the temperature dependence of the reaction or having an endothermic reaction causes negative feedback.

These two feedback mechanisms can be present simultaneously. They can also be coupled, i.e. a pressure dependent reaction which is exothermic. Note that normal attenuation mechanisms are still present and can cause an absolute decrease in sound intensity, with propagation distance, even when positive feedback is present.

In the following the general formalism of non-equilibrium chemical dynamics necessary to treat sound propagation in a chemically reacting mixture is described. This treatment is available in the cited literature so only the basic physics, major conclusions, and details useful to future students will be included. In practice, all computations were performed using a program written by Professor Gilbert[13]. Next, mechanisms for attenuation are identified and described only to the detail required for consistency. A program written by Professor Shields[17] (see appendix A) was used for this calculation with a modification to allow viscosity to be computed as a function of temperature for a ternary mixture.

General Formalism for Non-Equilibrium Thermodynamics

Equations needed to describe chemical amplification are presented in this section. The following is taken, in large part, from Reference 18.

Consider the reaction

$$2H_2 + O_2 \rightarrow 2H_2O \tag{2}$$

which is the form

$$2A_1' + A_2' \rightarrow 2A_3'. \tag{3}$$

If this is the kth reaction being considered, the actual stoichiometric coefficients, $\eta_{\ell k}$, are $\eta_{1k} = -2$, $\eta_{2k} = -1$, and $\eta_{3k} = +2$. Eq. (3) can be written in summation form as

$$\sum_{\ell}^{s} \eta_{\ell k} A_\ell' = 0 \tag{4}$$

where $\sum^{s}$ indicates a summation over all species. In terms of grams, instead of moles, eq. (3) is

$$4A_1 + 32A_2 \rightarrow 36A_3 \tag{5}$$

where A_j represents one gram of species j. Reducing eq. (5) gives

$$A_3 - \frac{1}{9} A_1 - \frac{8}{9} A_2 = 0 \tag{6}$$

or

$$\sum_{i}^{s} \nu_{ik} A_i = 0 \tag{7}$$

where ν_{ik} is the mass weighted stoichiometric coefficient for the i^{th} species and k^{th} reaction. Let the progress variable of the k^{th} reaction, λ_k, be defined as the number of grams of reactant which have reacted per gram of original reactant. Then

$$d_k m_i = m\nu_{ik}d\lambda_k \tag{8}$$

where m_i is the total mass of species "i", m the total mass, and $d_k m_i$ the change in m_i caused by the k^{th} reaction. The total change in m_i, dm_i, caused by all the reactions is

$$dm_i = \sum_k^r d_k m_i = m\sum_k^r \nu_{ik}d\lambda_k. \tag{9}$$

Dividing eq. (9) by the total volume gives

$$d\rho_i = \rho\sum_k^r \nu_{ik}d\lambda_k \tag{10}$$

where ρ_i is the mass density species "i", and ρ the mass density.

If one considers only forward reactions then, for our example

$$\rho d\lambda_j/dt = \rho\xi_j = k_j\rho_1^2\rho_2 \tag{11}$$

where ξ_j is the degree of advancement of the k^{th} reaction, $\equiv d\lambda_j/dt$, and k_j is the rate coefficient of the j^{th} reaction in the forward direction. In general form,

$$\xi_j = \rho^{-1}k_j\rho_1{}^{-\eta_1}\rho_2{}^{-\eta_2} \tag{12}$$

or, in terms of mass fraction, c_j,

$$\xi_j = \rho^{-1}k_j c_1{}^{-\eta_1}c_2{}^{-\eta_2}\rho^{-\eta_1-\eta_2} = \rho^{(g_j-1)}k_j c_1{}^{-\eta_1}c_2{}^{-\eta_2} \tag{13}$$

where g_j is the molecularity of the j^{th} reaction. For reactions of any order

$$\xi_j = \rho^{(g_j-1)} k_j \sum_{i}^{s'} (C_i)^{-\eta_i} \tag{14}$$

where C_i is the mass fraction of the i^{th} reactant, and $\sum^{s'}$ the sum over all reactants.

Consider any extensive variable, θ, i.e. energy or mass. Let G be specific θ, θ per unit mass. Then

$$\theta = {}_v\int \rho G dv \tag{15}$$

where the integral extends over the entire system; and

$$\dot{\theta} = d/dt\, {}_v\int \rho G dv. \tag{16}$$

If the volume remains constant, the time derivative may be taken inside the integral giving

$$\dot{\theta} = {}_v\int \frac{\partial}{\partial t} (\rho G) dv. \tag{17}$$

An alternate expression for $\dot{\theta}$ can be derived. If a flow of θ is present at the surface of a volume, then the resulting change θ with time is $-{}_s\int \bar{J}_G \cdot d\bar{s}$, where $\bar{J}_G$ is the current density for the extensive variable θ, $\rho G \bar{v}$; and $\bar{v}$ is the center-of-mass velocity. If there are internal sources of θ, denoted ϕ_G, the resulting change in θ with time will be ${}_v\int \phi_G dv$. Thus,

$$\dot{\theta} = -{}_s\int \bar{J}_G \cdot d\bar{s} + {}_v\int \phi_G dv. \tag{18}$$

Equating the two expressions for $\dot{\theta}$ gives

$$_V\int\{\frac{\partial}{\partial t}(\rho G) + \nabla\cdot\bar{J}_G - \phi_G\}dv = 0, \tag{19}$$

and since the volume was arbitrary

$$\frac{\partial}{\partial t}(\rho G) + \nabla\cdot\bar{J}_G - \phi_G = 0. \tag{20}$$

For future reference, let the partial specific θ, $\tilde{G}_i$, be defined by

$$\tilde{G}_i \equiv (\frac{\partial\theta}{\partial m_i})_{T,p,m_\ell,l\neq i}. \tag{21}$$

Applying eq.(20) to mass conservation of species "i" gives

$$\frac{\partial}{\partial t}\rho_i + \nabla\cdot\bar{J}m_i = \phi m_i \tag{22}$$

where $\bar{J}m_i$ is the mass current density of the i^{th} species, $= \rho_i\bar{v}_i$, $\bar{v}_i$ the velocity of the i^{th} species, and ϕm_i the source potential of the i^{th} species, $=\rho\sum_k^r \nu_{ik}\ \xi_k$. Summing eq. (22) over all species yields

$$\dot{\rho} + \rho\nabla\cdot\bar{v} = 0 \tag{23}$$

Eq. (22) can also be expressed in terms of mass fraction

$$\rho\dot{C}_i + \nabla\cdot\bar{j}_i = \rho\sum_k^r \nu_{ik}\ \xi_k \tag{24}$$

where $\bar{j}_i$ is the diffusion current density, $\rho_i(\bar{v}_i-\bar{v})$. Assuming no diffusion, eq. (24) becomes

$$\dot{C}_i = \sum_k^r \nu_{ik}\ \xi_k. \tag{25}$$

Applying eq. (20) to the x-component of momentum yields

$$\frac{\partial}{\partial t}(\rho\bar{v}_x) + \bar{v}\ (\bar{J}_{mom,x}) = \rho\bar{X}_x + (\nabla\cdot\underline{\sigma})_x \tag{26}$$

where $\bar{J}_{mom,x}$ is the x-component of momentum current density, $= \rho\bar{v}_x\bar{v}$; $\bar{X}_x$ the x-component of external force per unit volume; and $\underline{\sigma}$ the stress tensor. Combining eq. (26) with its y- and z- counterparts gives

$$\frac{\partial}{\partial t}(\rho\bar{v}) + \nabla\cdot(\rho\bar{v}\bar{v}) = \rho\bar{X} + \nabla\cdot\underline{\sigma} \tag{27}$$

and, using conservation of mass,

$$\rho\dot{\bar{v}} = \rho\bar{X} + \nabla\cdot\underline{\sigma}. \tag{28}$$

Assuming no external forces and using the stress tensor for homogeneous, isotropic fluids, eq. (28) can be written

$$\rho\dot{\bar{v}} = -\nabla p + \eta\nabla^2\bar{v} + (\tfrac{1}{3}\eta + \phi)\nabla(\nabla\cdot\bar{v}) \tag{29}$$

where η is the coefficient of shear viscosity, and ϕ the coefficient of bulk viscosity. Applying eq. (20) to entropy gives

$$\rho\dot{S} = \Phi/T - \nabla\cdot\bar{j}_s \tag{30}$$

where S is the specific entropy; Φ/T the source potential of entropy; and $\bar{j}_s$ the entropy flux caused by diffusion and heat flow. Φ is caused by viscous flow, chemical reactions, isothermal diffusion and heat flow. Fitts[18] calculated Φ, and by using conversation of mass and eq. (30), obtained the following

$$\rho K' C_v \dot{p} = \rho C_p \nabla\cdot\bar{v} - \sum_{j}^{r} \rho\xi_j(\beta\Delta H_j - \rho c_p \Delta V_j) \tag{31}$$

and

$$\rho K' C_v \dot{T} = -\beta T \nabla\cdot\bar{v} - \sum_{j}^{r} \rho\xi_j(K'\Delta H_j - \beta T\Delta V_j) \tag{32}$$

where $\Delta H_k = \sum_i^s \nu_{ik}\tilde{H}_i$, $\Delta V_j = \sum_i^s \nu_{ij}\tilde{V}_i$, $K' = \frac{-1}{V}(\frac{\partial V}{\partial p})_{T,M}$, and $\beta = \frac{1}{V}(\frac{\partial V}{\partial T})_{p,m}$. Eqs. (31) and (32) were derived using the following assumptions:

1. adiabatic conditions, $\nabla \cdot \bar{q} = 0$
2. no diffusion, $\bar{j}i = 0$
3. homogeneous, isotropic fluid with bulk and shear viscosities independent of gradients.

The necessary acoustic relationships follow from the conservation equations. It will be assumed that no chemical reactions are occurring and that, except for thermal conduction, no attenuation mechanisms are present. Attenuation will be included in later sections. With these assumptions, eq. (31) becomes

$$\dot{p} = -(c_p/c_v K')\nabla \cdot \bar{v} \tag{33}$$

For plane waves propagating in the x-direction in an ideal gas, eq. (33) reduces to

$$\dot{p} = -(c_p/c_v K')p\partial\bar{v}_x/\partial_x \tag{34}$$

where the difference between the substantial derivative, d/dt, and the time derivative, ∂/∂t, is second order and has been ignored. With the same assumptions as those used to obtain eq. (34), eq. (32) becomes

$$\frac{\partial}{\partial t} T = -p(\rho c_v)^{-1}\partial\bar{v}_x/\partial_x, \tag{35}$$

eq. (23) becomes

$$\frac{\partial}{\partial t}\rho + \rho\frac{\partial}{\partial x}\bar{v}_x = 0, \tag{36}$$

and eq. (28) becomes

$$\rho \frac{\partial}{\partial t} \bar{v}_x = (\nabla \cdot \underline{\sigma})_x . \tag{37}$$

Writing the stress tensor as

$$\underline{\sigma}_{ij} = -p\delta_{ij}, \tag{38}$$

eq. (37) simplifies to

$$\frac{\partial \bar{v}_x}{\partial t} = -(\frac{1}{\rho}) \frac{\partial}{\partial x} p . \tag{39}$$

So far, we have developed acoustic and chemical relationships between pressure, center-of-mass velocity, temperature, and mass fractions. These expressions have been combined by Gilbert et al.[5] as follows.

Let $\psi(x,t)$ be the space- and time-dependent vector of variables describing the system. The components of this vector are $(p, \bar{v}, T, c_i)$. Equations describing the system [eqs. (25), (29), (31), (32), (34), (35), (36), (39) and (40)] can be combined into one tensor equation

$$\frac{\partial}{\partial t} \psi = F[\psi] + B[\psi] \frac{\partial}{\partial x} \psi \tag{40}$$

where $F[\psi]$ is a nonlinear vector function describing the kinetics, and $B[\psi]$ a matrix function of ψ describing the acoustics.

The quantity, $\psi(x,t)$ can be written as the sum of $\psi^\circ(t)$, the part resulting from homogeneous evolution, and $\delta\psi(x,t)$, a small quantity resulting from acoustic perturbations. Homogeneous evolution is described by

$$\psi^\circ(t) = F[\psi^\circ] \tag{41}$$

or, without tensor notation, by

$$\dot{p}^\circ = -p^\circ (c_v^\circ)^{-1} \sum_{\ell}^{r} \xi^\circ [(T^\circ)^{-1} \Delta H_\ell^\circ - \rho^\circ c_p^\circ \Delta V_\ell^\circ] \tag{42}$$

$$\bar{v}^\circ = 0 \tag{43}$$

$$\dot{T}^\circ = -p^\circ (c_v^\circ)^{-1} \sum_{\ell}^{r} \xi^\circ [(p^\circ)^{-1} \Delta H_\ell^\circ - \Delta V_\ell^\circ] \tag{44}$$

$$c_i^\circ = \sum^{r} \nu_{i\ell} \xi^\circ . \tag{45}$$

Inhomogeneous evolution is described by eqs. (25) (29), (31), and (32). These four equations can be rewritten as

$$\frac{\partial}{\partial t} c_i = -\bar{v}_x \frac{\partial}{\partial x} c_i + \sum_{k}^{r} \nu_{ik} \xi_k \tag{46}$$

$$\frac{\partial}{\partial t} \bar{v}_x = -\rho^{-1} \frac{\partial}{\partial x} p - \bar{v}_x \frac{\partial}{\partial x} \bar{v}_x \tag{47}$$

$$\frac{\partial}{\partial t} p = -\bar{v}_x \frac{\partial}{\partial x} p + c_p \; p \; c_v{}^{-1} \frac{\partial}{\partial x} \bar{v}_x - p c_v{}^{-1} \sum_{j}^{r} \xi_k G_k \tag{48}$$

$$\frac{\partial}{\partial t} T = -\bar{v}_x \frac{\partial}{\partial x} T - (\rho c_v)^{-1} p \frac{\partial}{\partial x} \bar{v}_x - c_v{}^{-1} \sum_{j}^{r} \xi_j J_j \tag{49}$$

where the following assumptions and definitions have been made:

1. rate coefficients have an Arrhenius temperature dependence, $k_i = f_i' \exp(-E_i^A/RT)$, where f_i' is the frequency factor, and E_i^A the activation energy for reaction "i";
2. the molar, constant-pressure specific heats have the form $c_p^i = \alpha_i + \beta_i T + \eta_i T^{-2}$, where α_i, β_i, and η_i are the specific heat coefficients for the ith species;
3. $c_p = \sum_{i}^{s} c_p^i c_i M_i{}^{-1}$, where M_i is the molecular weight of species "i".
4. $q_i \equiv \alpha_i T + \frac{1}{2} \beta_i T^2 - \eta_i T^{-1}$

   $E_\ell \equiv E_\ell^A / RT^2 - T^{-1}(g_\ell - 1)$

$J_\ell \equiv \Delta H_\ell - p\Delta V_\ell$

$G_\ell \equiv T^{-1}\Delta H_\ell - \rho c_p \Delta V_\ell$

$M^\ell \equiv$ molecular weight on right-hand side of reaction "ℓ"

$\Delta H_\ell(T) = (M^\ell)^{-1}\{H_\ell(T = 298K) - \sum_i^s \eta_{i\ell}[q_i(T = 298K) - q_i(T)]\}$

$A_{i\ell} = \frac{\partial \xi_\ell}{\partial c_i} = \xi_\ell[-(\delta_{i\ell}\eta_{i\ell}/c_i) - (g_\ell - 1)M_i{}^{-1}\rho RTp^{-1}]$

$\eta_{i\ell} = \nu_{i\ell}M^\ell/M_\ell.$

Next, let the independent variables be composed of a homogeneous part plus a small inhomogeneous part, i.e. $p = p^\circ + \delta p$. Then the dependent variables can be written as a homogeneous part plus a Taylor series of inhomogeneous variables, i.e. $\rho = \rho^\circ + (\frac{\partial\rho}{\partial p})^\circ\delta p + (\frac{\partial\rho}{\partial T})^\circ\delta T + \sum_i^s (\frac{\partial\rho}{\partial c_i})^\circ\delta c_i + (\frac{\partial\rho}{\partial v_x})^\circ\delta\bar{v}_x$, where higher order terms have been neglected. Using this notation and neglecting higher order terms, eqs. (46) - (49) become

$$\frac{\partial}{\partial t}\,\delta c_i = \delta T \sum_k^r \nu_{ik}E_k^\circ\xi_k^\circ + (\delta p^\circ)^{-1}\sum_\ell^r(g_\ell - 1)\xi_\ell^\circ\nu_{i\ell} + \sum_j^s \delta c_j \sum_k^r \nu_{ik}A_{jk} \tag{50}$$

$$\frac{\partial\delta}{\partial t}\,\bar{v}_x = 0 \tag{51}$$

$$\begin{aligned}\frac{\partial}{\partial t}\,\delta p = {} & \delta p[-(c_v^\circ)^{-1}\sum_\ell^r g_\ell\xi_\ell^\circ G_\ell^\circ] + \delta T(-c_v^\circ)^{-1}\{p^\circ\sum_\ell^r[G_\ell^\circ\xi_\ell^\circ \\ & + (T^\circ)^{-2}(\Delta H_\ell - T\,\frac{\partial}{\partial t}\,\Delta H_\ell)^\circ - \rho^\circ\Delta V_\ell^\circ(\frac{\partial c\ell}{\partial t})^\circ]\} \\ & - c_v^\circ\dot{p}^\circ(\partial c_v/\partial T)^\circ\delta T + (-c_v^\circ)^{-1}\sum_k^s\delta c_k\{p^\circ\sum_\ell^r[G_\ell^\circ\;A_{k\ell} \\ & + \xi_\ell^\circ\Delta V_\ell^\circ M_k{}^{-1}\rho^\circ(c_p^\circ/\gamma^\circ - c_p^k)]\} - c_v^\circ\dot{p}^\circ\sum_i^s\delta c_i c_p^i M_i{}^{-1}\end{aligned} \tag{52}$$

$$\begin{aligned}\frac{\partial}{\partial t}\,T = {} & -(c_v^\circ)^{-1}\{8T[(\sum_j^r\xi_j^\circ(\frac{\partial}{\partial t}\,\Delta H_\ell)^\circ - p^\circ(T^\circ)^{-1}\Delta V_\ell^\circ + J_\ell^\circ E_\ell^\circ) - (c_v^\circ)^2\dot{T}^\circ] \\ & + \delta p[\sum_\ell^r J_\ell^\circ(g_\ell - 1)(p^\circ)^{-1}\xi_\ell^\circ + \sum_i^s\delta c_i[\sum_\ell^r A_{i\ell}^\circ J_i^\circ - (c_v^\circ)^2 C_p^i M_i{}^{-1}\dot{T}^\circ]\}\end{aligned} \tag{53}$$

where the homogeneous parts have been eliminated using eqs. (41) - (45). Eqs. (50) - (53) can be written in matrix notation as

$$\frac{\partial}{\partial t}\,\delta\psi = Q(\psi^\circ)\delta\psi \tag{54}$$

where $Q(\psi^\circ)$ is a matrix whose elements are found by solving the equation for homogeneous evolution, (41). A numerical solution[6] of eqs. (41) and (54), written by Professor Gilbert, was used to predict sound amplification for our experiments. The solution uses the Gear method[19] of solving stiffly coupled differential equations. Another study of sound amplification in Cl_2-H_2 gas-phase chemically reacting mixtures has been published by Toong et al.[7-9]; it will be considered briefly. While similar to Gilbert's solution, Toong's derivation neglects viscosity and thermal conductivity; however, this simplification allows for analytical solutions. Thus, clear insights concerning acoustic-chemical interactions are possible. Toong[8] presents a useful equation for comparing sound attenuation with and without chemical amplification

$$\Delta\alpha = (2\gamma T)^{-1} dT/dt[m' + (E^A/RT)(\gamma-1)(T_i/T) + \gamma] \tag{55}$$

where T_i is the initial temperature and m' the order of the reaction. Both Gilbert and Toong's solutions are compared to our experimental results.

Attenuation

In order to predict the absolute sound amplitude in a reacting mixture the standard attenuation mechanisms must also be considered. These losses are caused by viscosity, thermal conductivity, mass diffusion, and vibrational and rotational relaxation. In addition, there are losses associated with sound propagation inside a tube. Attenuation resulting from viscosity and thermal conductivity is termed classical attenuation. The classical attenuation coefficient is given by

$$\alpha_{cL} = 2\pi^2/\rho a^2 (\tfrac{4}{3}\eta + \frac{\gamma-1}{\gamma}\frac{k}{cv})f^2 \qquad (56)$$

where α_{cL} is the exponential decay constant for sound pressure amplitude, i.e. $A\exp(-\alpha x)$ where x is the propagation distance. Beginning with the conservation equations for mass, energy, and momentum, Kirchhoff[21] obtained an algebraic equation for the propagation constant for radially summetric waves. Kirchhoff assumed that particle velocity and sound temperature were zero at the tube wall. Henry[22] pointed out that these conditions might be inadequate, owing to the temperature jump and slip velocity at the tube wall. Shields[23] has modified Kirchhoff's equations to include temperature jump and slip velocity. The corrected equations were solved numerically using a computer program *developed* by Shields which is described in Reference 24. The physical constants for our waveguide were obtained from Shields[25]. Reflection coefficients at the ends of the tube were needed to correct for losses upon reflection. The coefficients were measured at room temperatures. The temperature dependence of reflection coefficients is weak[24,26] and therefore was not considered; endplate temperature varied only slightly during our experiments.

When a density gradient exists in a mixture of gases, there will be a greater flow of light molecules, relative to their concentration, than of heavy molecules. This results because, for a given temperature, lighter molecules are traveling faster than heavy molecules. The results is a periodic unmixing of the gas, offset by irreversible diffusion, which results in an energy loss of the sound wave. This effect is additive to that of classical absorption and has an attenuation coefficient given by

$$\alpha_{diff} = (\pi^2\gamma f^2/a^3\rho^2) \sum_{i,j,k}^{s} x_j s_k (m_j - m_k) x (m_j D_{ij} - m_k D_{ik}) \qquad (57)$$

where D_{ij} is the multicomponent diffusion coefficient for particle "i" and "j", m_i the mass of the i^{th} particle. For the gas mixtures used in this study, attenuation resulting from diffusion was much smaller than those caused by tube losses or vibrational relaxation. The computer programs which calculated attenuation did not consider attenuation resulting from diffusion.

When sound propagates through polyatomic gases the compressions and rarefactions involve a redistribution of energy between the various modes of excitation; this includes vibrational and rotational modes. At sufficiently high frequencies, the period of fluctuation becomes shorter than the time required for the redistribution of energy into the various modes. When this occurs the compressions and rarefactions are no longer reversible and attenuation results. Since rotational energy levels are closely spaced near room temperature for Cl_2, H_2, and SF_6, a single relaxation time can be used[27] to describe rotational relaxation. The resulting absorption coefficient, for the frequencies we used, is[27]

$$\alpha_{rot} = \sum_{i}^{s} \{[N x_i' \pi f^2 (d_i/2) R(\gamma-1)]/(f_{r,rot} c_p^{\infty} a)\} \qquad (58)$$

where d_i is the number of rotational degrees of freedom, i.e. 2 for H_2, Cl_2, 3 for SF_6; x_i the fractional number of molecules of species "i"; N is the total number of molecules; and $f_{r,rot}$ the frequency associated with relaxation of rotational modes. Since α_{rot} and α_{CL} have the same frequency dependence, rotational relaxation can be included by modifying the classical attenuation coefficient[26].

Two vibrational attenuation mechanisms were considered in our calculations: collisions which relax/excite the first vibrational level in Cl_2; and collisions which relax/excite vibrational levels of SF_6. H_2 and upper Cl_2 vibrational states are not considered because at lower temperatures they are rarely excited. The first mechanism is especially simple because it involves only one vibration-translation (v-t) process and can be considered a pseudo-first-order chemical reaction[5]

$$Cl_2(v=0) \rightleftarrows Cl_2(v=1) \tag{59}$$

In general, collisions which exchange multiple quanta of energy, in v-t and v-v processes, must be considered to predict vibrational attenuation. For example, if A and B collide, A may loose two quanta of vibrational energy and B receive one quantum of vibrational energy and some translational energy. This coupling between v-t and v-v processes complicates the problem[28,29] greatly; however, SF_6 has properties which simplify the problem. SF_6 has many vibrational levels which are excited even at low temperatures (~300K) but, the lowest level deexcites much slower than the others. This lowest level gating makes it possible to characterize SF_6 vibrational relaxation with one relaxation time[29], τ_{vt} . For frequencies such that $\omega\tau_{vt} << 1$, which includes the range we used,

$$\alpha_{vt}\lambda = \frac{2\pi^2 C_v}{C_o(C_o+1)} \left(\frac{f}{p}\right)(p\tau_{vt}) \tag{60}$$

where C_o is the constant volume specific heat for low frequencies, and C_v is the contribution to C_o resulting from vibrational relaxation. Eq. (60) is multiplied and divided by pressure, p, because $(p\tau_{vt})$ is pressure independent for binary-collision induced relaxation. The vibrational relaxation time, τ_{vt}, for a mixture of Cl_2-H_2-SF_6 is given by

$$\frac{1}{\tau_{vt}} = \frac{x'_{H_2}}{\tau_{vt,H_2}} + \frac{x'_{Cl_2}}{\tau_{vt,Cl_2}} + \frac{x'_{SF_6}}{\tau_{vt,SF_6}} \tag{61}$$

where τ_{vt,SF_6} is the vibrational relaxation time for pure SF_6; $\tau_{vt,j}$ is the vibrational relaxation time related to SF_6 in mixtures of "j". Equation (61) can be used to determine the constants τ_{vt,SF_6}, τ_{vt,Cl_2}, and τ_{vt,H_2} by determining τ_{vt} for a number of known concentrations, x'_{H_2}, x'_{Cl_2}, and x'_{SF_6}. The τ_{vt}[15] are found by measuring α_{total} for various pressures, frequencies, and concentrations of H_2 and Cl_2 in SF_6; substracting other attenuation terms to get α_{vt} for each set of parameters; and solving eq. (60) for τ_{vt}.

Reaction Details

Two SACERs were constructed for this investigation; one operated in a pulsed mode, the other in a cw mode. Both systems are characterized chemically by the following H_2-Cl_2 reactions[3,14]

$$Cl_2 + h\nu \rightarrow 2Cl \text{ (photo initiated dissociation)} \tag{62}$$

$$Cl + H_2 \rightleftarrows HCl + H \tag{63}$$

$$H + Cl_2 \rightarrow HCl + Cl \tag{64}$$

$$M + 2CL \rightleftarrows M + Cl_2 \tag{65}$$

$$Cl_2(v=0) \rightleftarrows Cl_2(v=1) \tag{66}$$

Where M represents SF_6 for the cw SACER, Ar for the pulsed SACER. The last "reaction" is a pseudo-first-order reaction which allows for Cl_2 vibrational excitement. The physical parameters associated with these reactions were obtained from references 5 and 6.

CHAPTER III

APPARATUS

Two systems were constructed for this investigation. The first was used for pulsed SACER experiments, the second for cw-SACER and attenuation experiments. A brief description of the systems will be given, followed by a more complete discussion of individual components.

Fig. (1) illustrates the acoustic and lighting equipment used for the cw experiments. The heart of the system was a cylindrical waveguide (1m x 3cm) with transducers at each end. The tube was made of Vycor which is UV-transparent. Three UV-fluorescent lamps surrounded the tube and provided UV-radiation needed to dissociate Cl_2. Aluminum slats supported the lamps and helped insure homogenous illumination of the Vycor tube. The acoustic waveguide and lamps were enclosed in an aluminum tube to increase UV-intensity inside (aluminum is an excellent UV-reflector). The entire system was covered with a light-tight cloth to protect the lab from UV-radiation and isolate the system from UV-radiation emitted by fluorescent lamps in the lab. A similar system was used for pulsed experiments (see fig. (2)). Intense flash lamps were used to dissociate Cl_2 at the start of each experiment. Unilluminated regions at each end of the tube generated acoustic pulses which propagated down the tube. Two microphones were used to monitor the amplitude of these pulses. The first microphone was mounted flush in one end of the tube, the second microphone was mounted near the other end of the tube. A

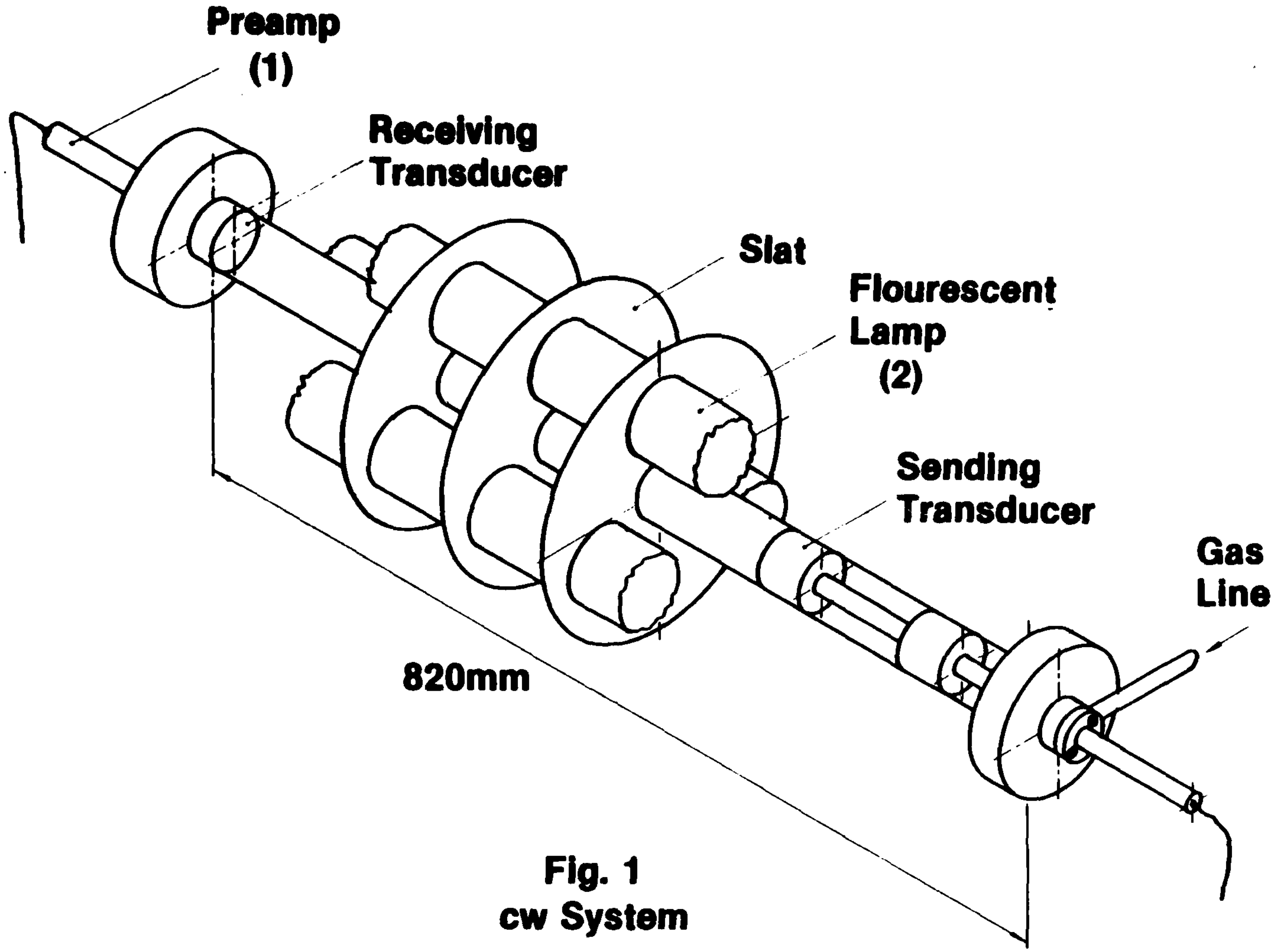

Fig. 1
cw System

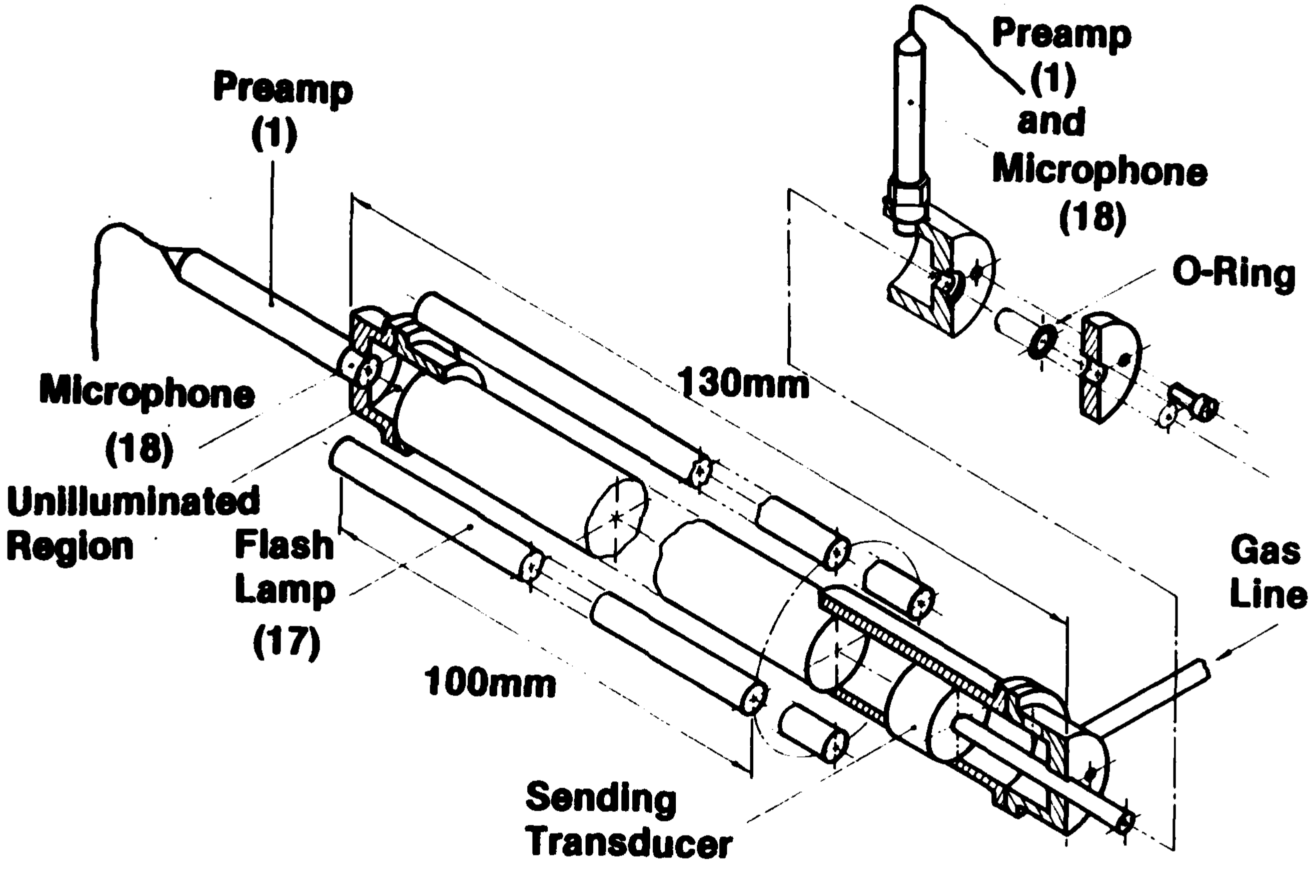

Fig. 2
Pulsed SACER

movable sending transducer was mounted opposite the first microphone, but was used only as a reflector because the intense acoustic pulses, generated by the unilluminated regions, masked tone bursts generated by the transducer. A LSI-11 based minicomputer (MINC system 11/23) was used for cw-SACER experiments to receive data, control experiment, and graph and analyze data. The computer was equipped with an A/D converter and digital out (DO) module. The A/D converter was used to digitize the signal from the receiver. The DO module generated digital pulses which controlled the sending transducer and equipment associated with fluorescent lamps. Attenuation measurements were made with the system used for cw experiments. The lamps were not needed for attenuation measurements. All experiments used research grade gases (Matheson Gas, $\geq 99.96\%$ pure) with the exception of H_2 used during attenuation measurements. Low impurity levels could be tolerated in H_2-SF_6 attenuation measurements because H_2 is generally more effective at relaxing vibrational modes in SF_6 than impurities.

Two solid dielectric capacitance transducers were used in the cw system (see fig. (3)). Both were constructed in our laboratory for this experiment. Each had a high voltage plate covered with 0.0127 mm Kapton which had an aluminum coating on the side away from the high voltage back plate. The aluminum coating and back plate formed a capacitor whose separation distance could be varied with acoustical pressure or applied voltage. One transducer was operated in transmitting mode, the other in a receiving mode.

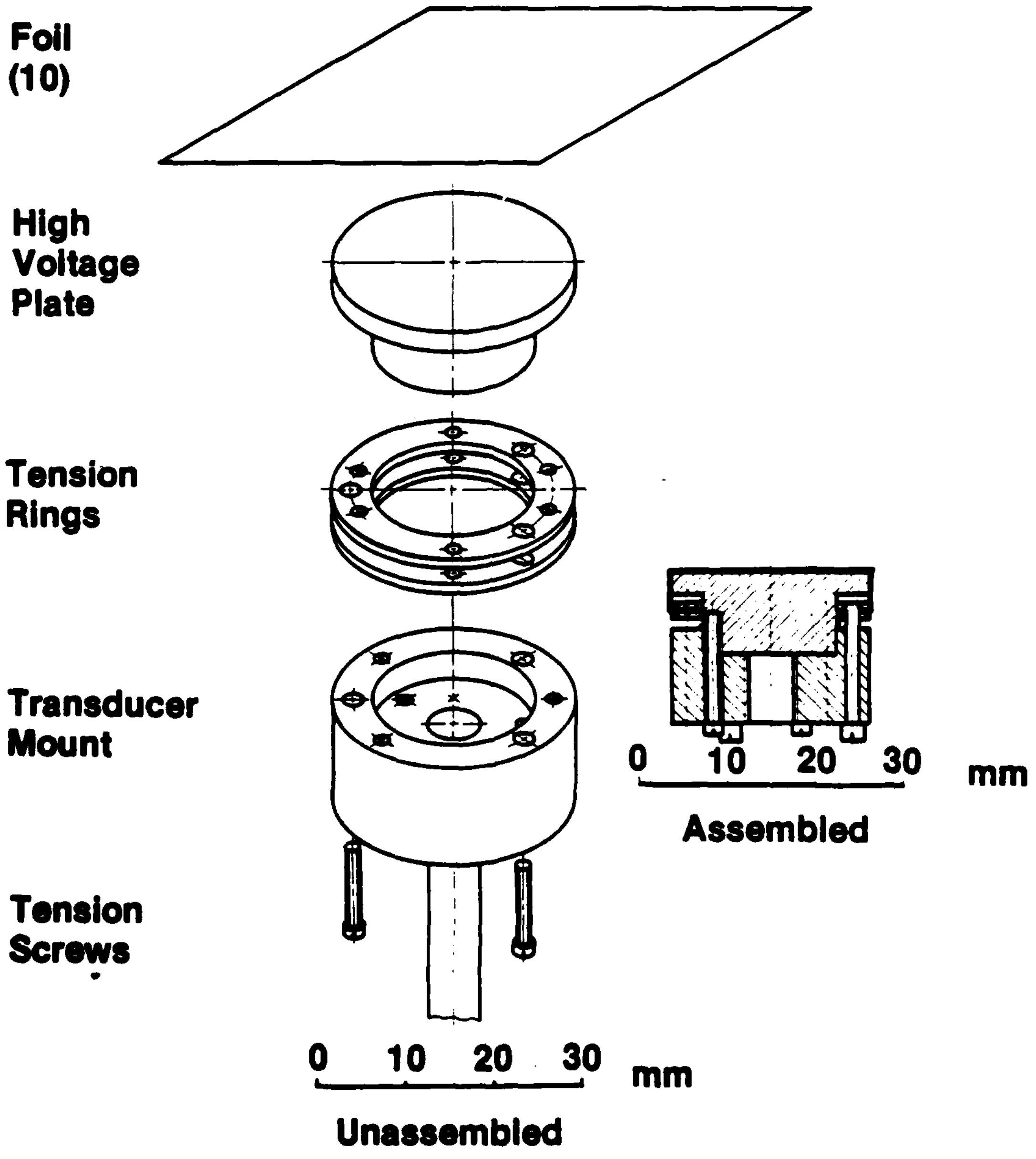

Fig. 3
Transducer For cw System

TABLE (1)

Equipment List

1. General Radio Company, Preamplifier Type 1560-p42
2. General Electric, Black Light no. F40BL
3. Hewlett-Packard, 3312A Function Generator for cw-SACER experiments; Hewlett-Packard, 200 CDR Wide Range Oscillator for attenuation experiments
4. Dynaco, Mark VI Amplifier
5. Electro Instruments, Inc., Precision Power Source no. 6303PS
6. General Radio Company, 1560-P62 Power Supply
7. Rockland, Dual Hi/Lo Filter no. 452
8. Eg&G Parc, 113 Pre-Amp
9. Each lamp had its own Regulated Power Supply:
    - Philbrick Researchers, R-600
    - Philbrick Researchers, R-300
    - Lambda, C-881M
10. Sheldahl, 0.0127 mm Kapton with aluminizing
11. Fluke, 1911-A Multi-Counter
12. Eico, 1064 Power Supply
13. Digital, minicomputer no. MNC11-FA, version 2.0, system 11/23, LSI-11 based
14. Albia Electronics, DM-6 Variable Power Supply
15. Xeon Corporation, Model A Power Supply
16. Xeon Corporation, Model C rf-Trigger
17. Xeon Corporation, 1 meter Micropulse Flash Lamp
18. Bruel & Kjaer, Condenser Microphone Cartridge Type 4149

For the transmitter, a force was applied to the aluminum coating by varying the potential between it and the high voltage plate. This force caused the Kapton to oscillate sending an acoustic signal down the tube. Two voltages were applied to the transmitter, a 200 volt bias which insured that the foil and back plate did not separate, and a ± 20 volt tone burst which caused the oscillations. The two voltages were combined with a voltage adder built in this lab (see appendix B). The sender was movable so the distance between transmitter and receiver could be changed.

Acoustical pressure variations on the receiving transducer caused the potential between aluminum coating and backplate to vary. A GenRad preamp/power supply combination was used with the receiver to apply a 200 volt bias and detect the ac voltage caused by acoustic signals. The receiver sensitivity was controlled by decreasing the active area of the high voltage plate (see fig. (4)). Fig. (5) illustrates additional signal conditioning electronics associated with both transducers.

The pulsed system was equipped with two 1.27 cm, B&K condenser microphones (see fig. (2)). One microphone was mounted flush in an endplate, the other was mounted near the other endplate with its active surface parallel to the tube's axis. Both were powered by GenRad preamp/power supply combination like the one described for the cw system. A sending transducer was mounted in the other endplate; the sound it generated was not intense enough to be used for the pulsed experiments.

Several constraints were placed on the UV-radiation sources used for cw operation. They had to start quickly, relative to the relaxation

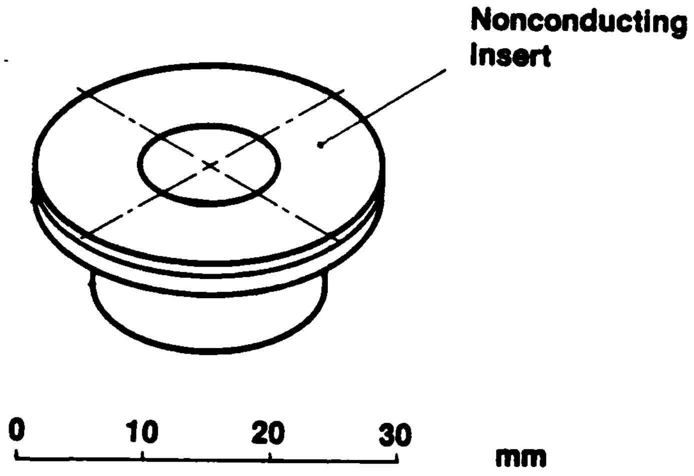

Fig. 4
Reduced Area High Voltage Plate

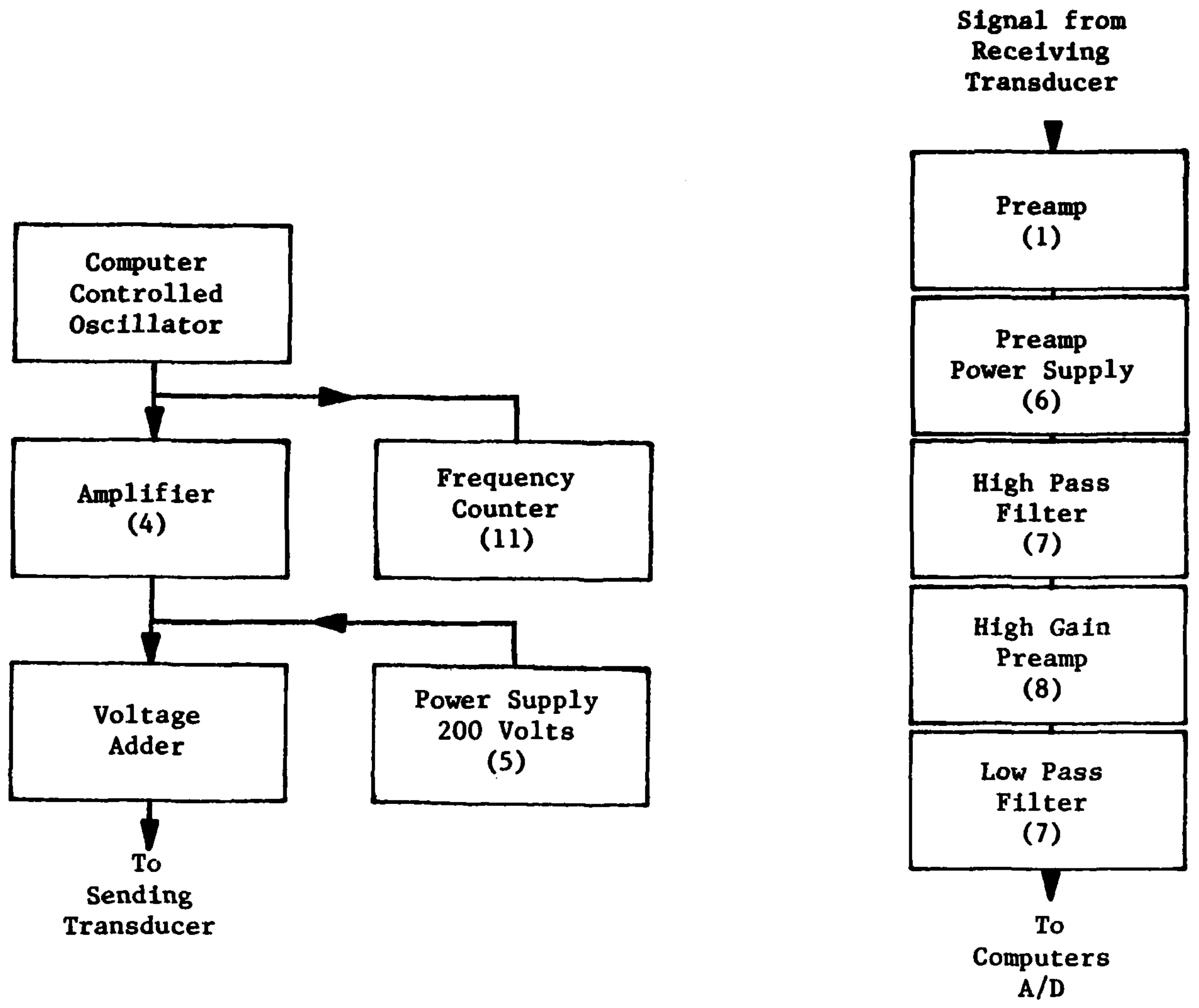

Figure 5

Electronics for Transducers in cw System times of the chemical reactions, and not cause large electrical disturbances which would be picked up by the receiver preamp. To this end, a complicated procedure was developed to start the UV-flourescent lamps (see fig. (6)):

1. 300 volts dc was applied across the lamps
2. 12 volts dc was supplied to glow one filament for 1/2 sec.
3. the lamps started when the wire, wrapped around the lamps, and the slats were shorted to the 300 volt terminal; the wire and slats were "floating" before the shorting process.

After starting, the lamps drew one amp each. Due to the large power requirement, each lamp was powered separately. Timing for lamp starting and transducer activation was provided by the minicomputer. The UV-flash lamps used for the pulsed experiments had to dissociate the Cl_2 quickly, compared to the time scale of the chemical reactions, at the beginning of each experiment. The four cylindrical flash lamps (1m x 1cm) were powered by a bank of capacitors. They were triggered with a rf-oscillator (see fig. (7)). The lamps were flashed at 10 kvolts with a 30 kvolt trigger. Pulse duration was estimated by the supplier (Xenon, Inc.) to be 10 μsec. The intensity of the UV-flash could be changed by varying the number of capacitors in the power supply.

As mentioned earlier, the cw-SACER experiments were controlled by a MINC-11/23 computer system manufactured by Digital Equipment Corporation. The system included lab modules which digitized data and provided digital signals to activate lab equipment. Fig. (8) illustrates the computer and related equipment. The digital output (DO) module sent digital pulses,

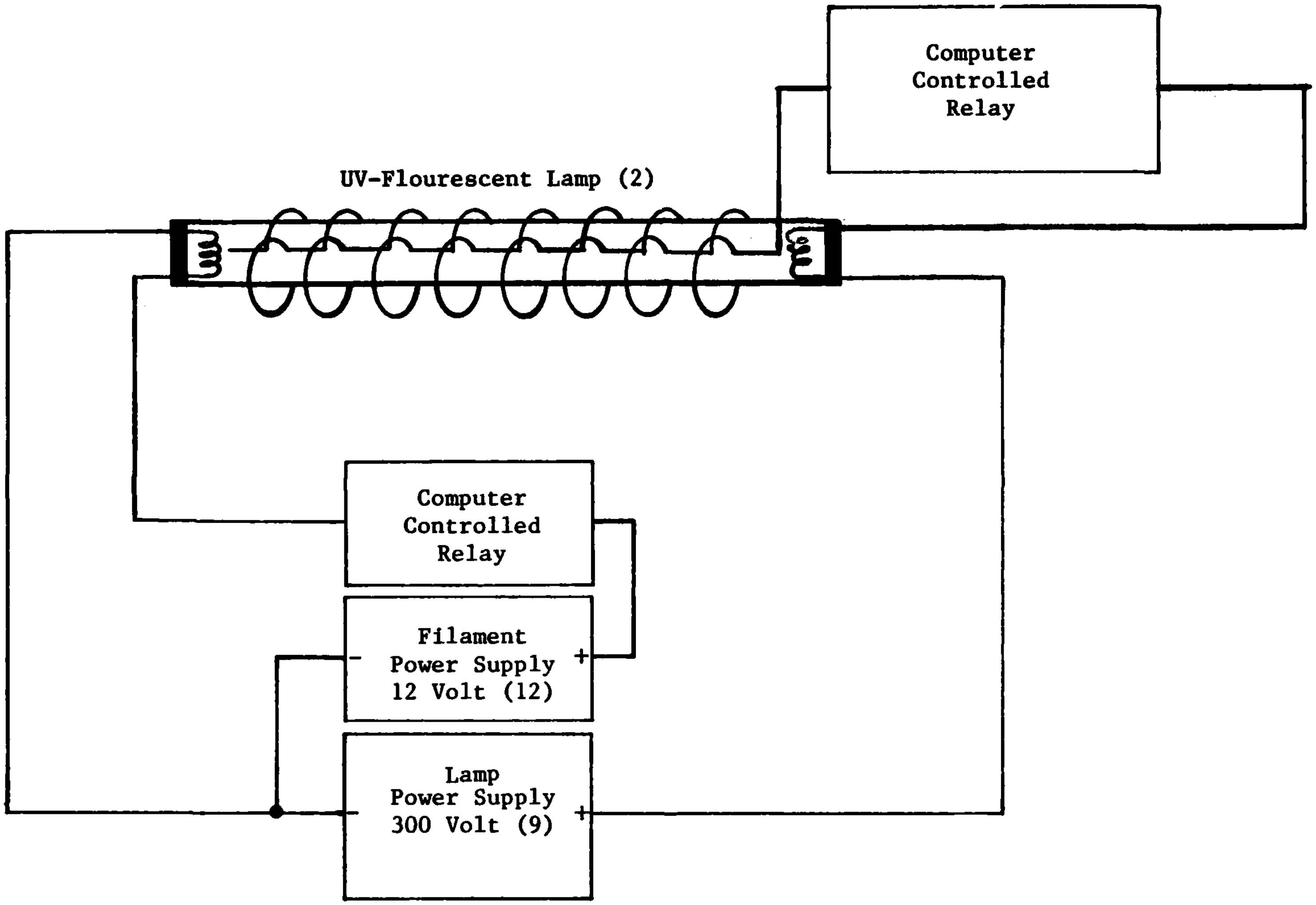

Figure 6

Electronics for UV-Lamps with cw-SACER

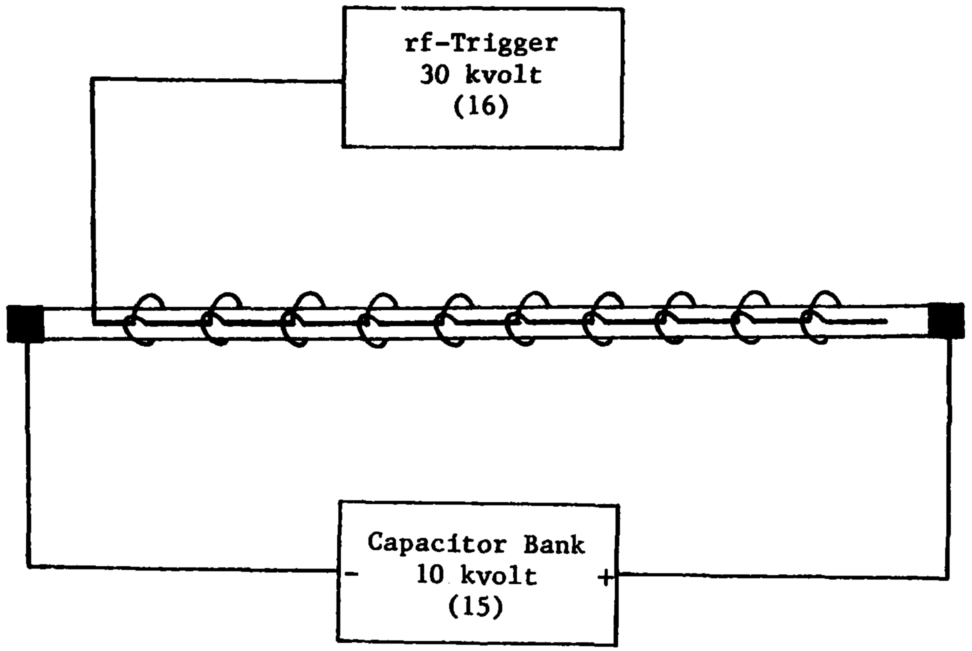

Figure 7

Electronics for UV-Flash Lamps Used in Pulsed System

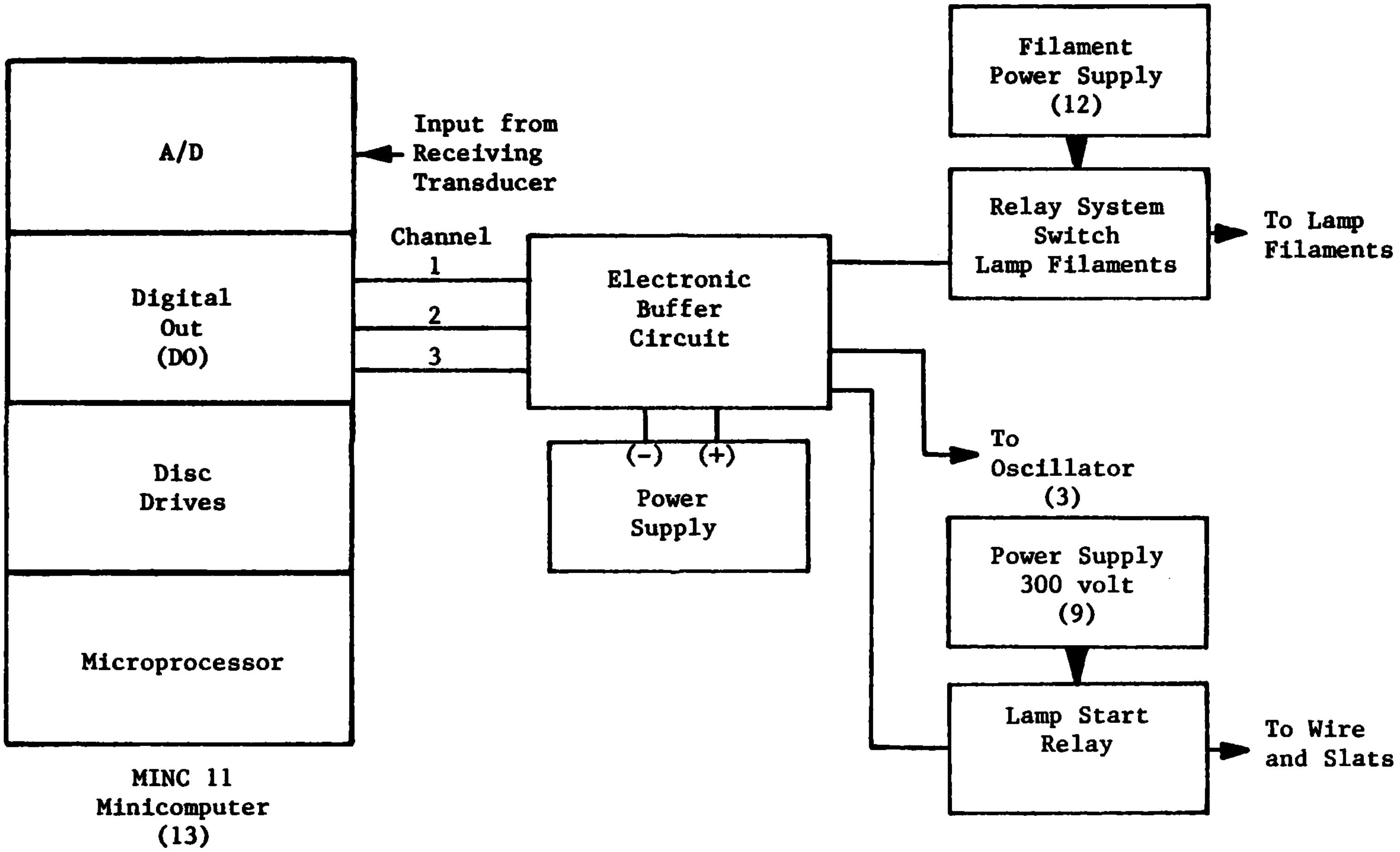

Figure 8

Minicomputer System Used to Control cw-SACER of variable length and time, to the electronic buffer equipment. The buffer equipment insured that DO signals were impedance-matched with later equipment and that electronic noise, caused by the SACER, did not get sent back to the computer. Three DO channels were used to control the function generator, current to lamp filaments, and voltage applied to the wire wrapped around the lamps. The A/D converter was used to digitize the amplified signal from the receiving transducer.

During cw-SACER experiments the amplitude of a tone burst was monitored as it propagated through a reacting gas mixture. UV-lamps continuously dissociated Cl_2 allowing the reaction to proceed slowly until all the H_2 was used (approximately 100 msec). The experiments were conducted as follows:

1. Using the law of partial pressures, a stainless steel storage tank was filled with enough Cl_2, H_2, and SF_6, in the desired concentrations, to conduct several experiments. The gases were then allowed to mix one day for each atmosphere of pressure in the tank.
2. After mixing, but before the SACER tube was filled with gas, the lamps were turned on and off once to insure proper starting during later operation.
3. 300 volts was applied across the lamps without starting them.
4. The SACER tube was filled with mixed gas.
5. The computer then controlled the SACER in this order:
   -glow lamp filaments 1/2 sec to insure proper lamp starting
   -then start digitizing data from receiving transducer and start lamps by changing the poten- of the wire coiled around the lamps.
   -activate sending transducer to send 4 msec tone burst at predetermined time after lamp start
   -stop digitizing 150 msec after lamp start.
6. After each run the lamps were turned off and the gases pumped out of the SACER tube.

7. Steps 2-6 were repeated at approximately half hour intervals until the storage tank was depleated.

During each pulsed experiment, UV-flash lamps dissociated Cl_2 in the SACER tube. This began the reaction and caused the pressure to rise rapidly everywhere inside the tube except for small unilluminated retions at each end of the tube. The increasing pressure caused gas to expand into the unilluminated regions. This expansion led to pulses which propagated down the tube. Microphones monitored the amplitude of the pulses as they propagated inside the tube. Because all the Cl_2 was immediately dissociated, the reactions only lasted approximately 10 msec. Pulsed SACER experiments were conducted as follows:

1. The SACER tube was filled with the proper mixture of Cl_2, H_2, and Ar. The gases were then allowed to mix thoroughly (at least four hours).
2. The capacitors were charged and then used to flash the lamps. The microphone outputs were stored on a fm-recorder and later analyzed.

In determining the vibrational relaxation time for gas mixtures used during cw-SACER experiments, a set of attenuation experiments were conducted. During attenuation experiments, the amplitude of the first reflection was measured for different transducer separations. Experiments were conducted at various pressures, frequencies, and Cl_2 and H_2 concentrations in SF_6. The concentrations were 10, 20, and 50 percent H_2, 10 and 20 percent Cl_2, and pure SF_6; the frequencies ranged from 1.5-50kHz; and the pressures ranged from 25-400 torr. These steps were followed for each attenuation experiment:

1. A stainless steel storage tank was filled with enough SF_6 and Cl_2 or H_2, in the desired partial pressures, to fill the tube several times.
2. After mixing the gases for 24 hours, the SACER tube was filled to the highest pressure used in attenuation experiments.
3. At the largest transducer separation distance, the pressure amplitude of the first received tone burst was measured for each frequency.
4. The distance between transducers was reduced and step 3 repeated.
5. Step 4 was repeated approximately twelve times.
6. The pressure was lowered and steps 3-5 repeated. Because a small amount of leakage occurred around the movable transducer's mount, the system was periodically evacuated and refilled to ensure the gas mixture was not contaminated.

CHAPTER IV

EXPERIMENTAL RESULTS

Pulsed SACER

Pulsed SACER experiments were begun by generating Cl atoms with a very short UV pulse, then allowing reactions (63-66) to go to completion modulated by an acoustic signal. The acoustic signal resulted from unilluminated regions in the tube and was monitored with two microphones. Electronic filters were used to examine individual frequency bands found in the acoustic signal. A frequency band centered about 2kHz was examined for amplification.

Experimentally, the amounts of Cl_2, H_2, and Ar initially in the system could be controlled. Also, varying the flash intensity gave some control over the initial concentration of atomic chlorine. One of the first tasks was to determine the optimum conditions for observing sound amplification. It was necessary to consider the chemical reactions (63-65) and the attenuation mechanisms present. A computer program written by Gilbert et al.[6] was used to include the chemical reactions; a program developed by Shields[23] was modified to compute tube and classical attenuation as a function of frequency, gas composition, temperature, and pressure. These two programs were used to solve for signal strength as a function of time for various reacting gas mixtures.

Ideally, we would like to have computed amplication for many sets of initial conditions; however, since each set required about 30 CPU minutes (Dec system 1077) only 60 sets were considered. From the computer outputs we were able to develop a physical feel for the competing mechanisms. For example, Table (2) illustrates the effect of varying H_2 concentration. For these calculations, it was assumed that 0.0005 atm of Cl_2 were dissociated by the UV flash. At low H_2 concentrations, the primary mechanism for amplificiation is recombination of Cl_2. In the absence of tube and classical losses, after 3msec, this mechanism would result in a gain of 1.7. Attenuation decreases this to 1.5 and 0.75 at 1m and 2m respectively. As the H_2 concentration is increased, reaction (64) becomes more important and the amplification increases up to about 8 after 1m because reaction (64) is highly exothermic. Greater H_2 concentration does little to increase amplification.

Table (2) also illustrates that, for the case of varying H_2 concentration, large amplification is accompanied by large overpressure. This trend occurred repeatedly in our computer simulations. The microphones used in the pulsed system could only withstand an overpressure of 0.03 atm which limited allowable initial conditions and expected amplification.

In pulsed SACER experiments, after the lamps dissociate Cl_2, the pressure in the illuminated region increases due to the dissociation and the subsequent heating from exothermic reactions. The increased pressure in the illuminated region expands into the unilluminated regions at each end of the tube. When the expansion reaches the microphones, the pressure rapidly increases. The positive pressure pulse is followed by a decrease in pressure. The lower pressure duration is about X_n/c where c is the speed of sound and X_n is the length of the unilluminated section.

TABLE (2)

Pulsed SACER Results

Total Pressure = 0.025 atm

Concentrations in atm			Overpressure (atm)		Amplitude (initially 1)		
[Cl_2]	[H_2]	[Ar]	1 ms	40 ms	3 ms	1m	2m
.005	.0005	.0195	.049	.065	1.7	1.5	.75
.005	.001	.019	.068	.084	7.5	3.7	1.8
.005	.002	.018	.106	.120	16	8.3	4.3
.005	.003	.017	.143	.155	16.5	8.3	4.3

This pattern is repeated as the pressure pulses bounce back and forth in the tube. An example of this type of signal is illustrated in figure (9). By filtering the signal, the amplitude of one band of frequencies can be observed. When this is done, a series of decaying pulses is observed; each pulse being similar to a sine wave with a gaussian envelope. It is the change in amplitude of these pulses that is examined for amplification.

The system had two microphones which detected the pressure changes. One microphone was mounted flush in the end opposite the sending transducer, the other was mounted, with its face parallel to the axis of the sound tube, at the same end as the sending transducer. These microphones will be referred to as mike 1 and mike 2 respectively.

For the optimum mixture listed above, the first burst arrives at mike 1 about 2msec after the flash. The second burst has reflected off the opposite end, traveled back down the tube and arrives about 7msec after the flash. The third burst is the same as the first after traveling to mike 2, reflecting off the sending transducer and returning. Subsequent pulses correspond to reflections back and forth in the tube.

For the purpose of the following arguments, a numbering system has been constructed to keep track of these bursts. The first burst received at mike 1 is denoted B_1^1, the second B_2^1, the third B_3^1, etc. At mike 2, the same bursts are referred to as B_0^2, B_1^2, B_2^2, etc. In this way, an odd subscript refers to a burst which arrived first at mike 1. This means that B_1^1 is the same burst as B_1^2 but B_1^2 has traversed an additional 1m down the tube to mike 2. The amplitude of B_1^1 will be denoted by A_1^1, etc.

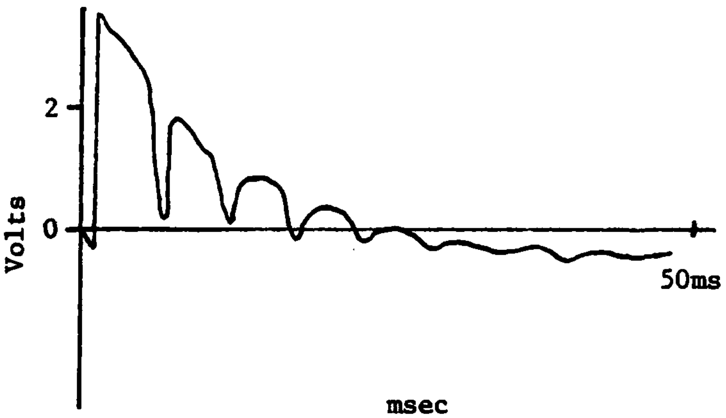

Figure 9

Unfiltered Output from Pulsed SACER Experiment
Cl_2-4.6 Torr; H_2-0.7 Torr; Ar-4.2 Torr

Before discussing specific results, it should be noted that the ratio, A_1^1/A_2^1 has no particular significance by itself since this ratio is a function of the unilluminated volumes, on each end, which (for the mike 2 end) is variable. Further, since mikes 1 and 2 are mounted differently, the ratio A_0^2/A_1^1 has no significance. However, by comparing several experiments these ratios can provide information.

Figure (10) shows the signal strength at mike 1, on a log scale, versus propagation distance for Cl_2-Ar mixture. For a gas with no amplification, the points should lie along a straight line since the signal strength A is equal to $A_0 \exp(\alpha x - n\beta)$ where α is the absorption coefficient for the gas, β is the reflection coefficient, and n the number of reflections. As shown in figure (10), the points lie along a straight line indicating there is little if any amplification from the Cl_2-Ar mixture, as expected. Also note that although the points for the signal originating near mike 2 are offset in absolute magnitude, the decay rate is the same (to within the measurement accuracy). Figure (10) indicates that the 2kHz component of the pressure pulse originating near mike 2 begins at a level 1.15 greater than the pulse originating near mike 1.

Figure (11) illustrates the results of adding H_2 to the Cl_2-Ar mixture in the ratio, 0.077 atm Ar: 0.019 atm Cl_2: 0.003 atm H_2. The signal strengths for both microphones (obtained from oscilloscope traces of the filtered signals) are plotted on a log scale. At both microphone positions, the signal decreases logrithmically with distances, the recorded amplitude is well below the straight line extrapolation. This suggests that there is a time over which the signal is amplified. By

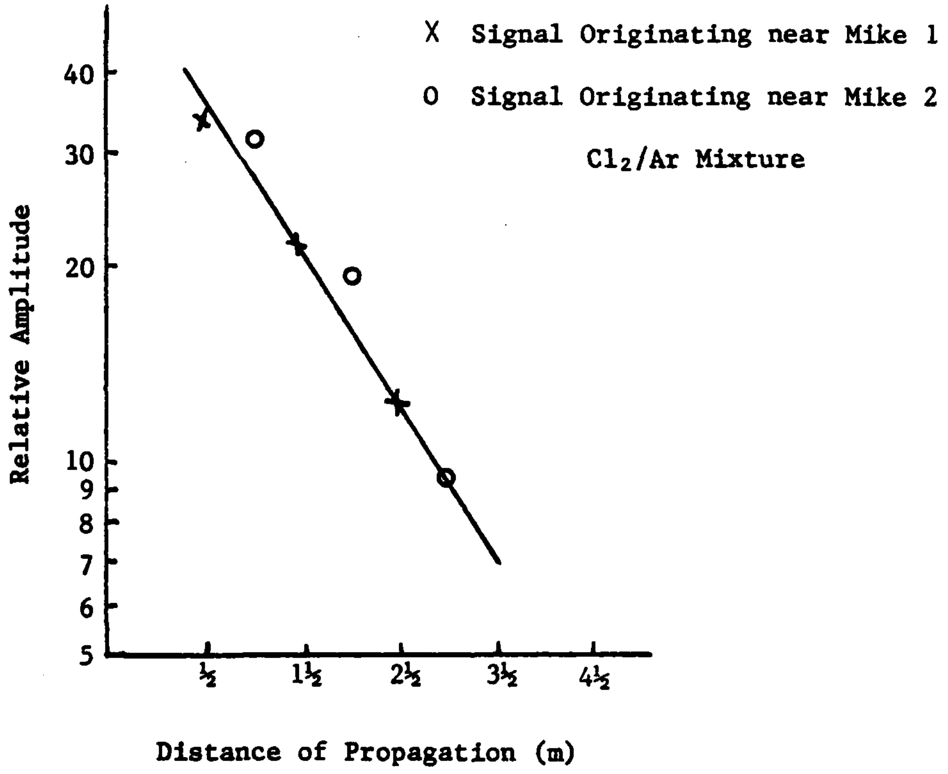

Figure 10

Signal Strength Versus Propagation Distance for 2kHz Signal

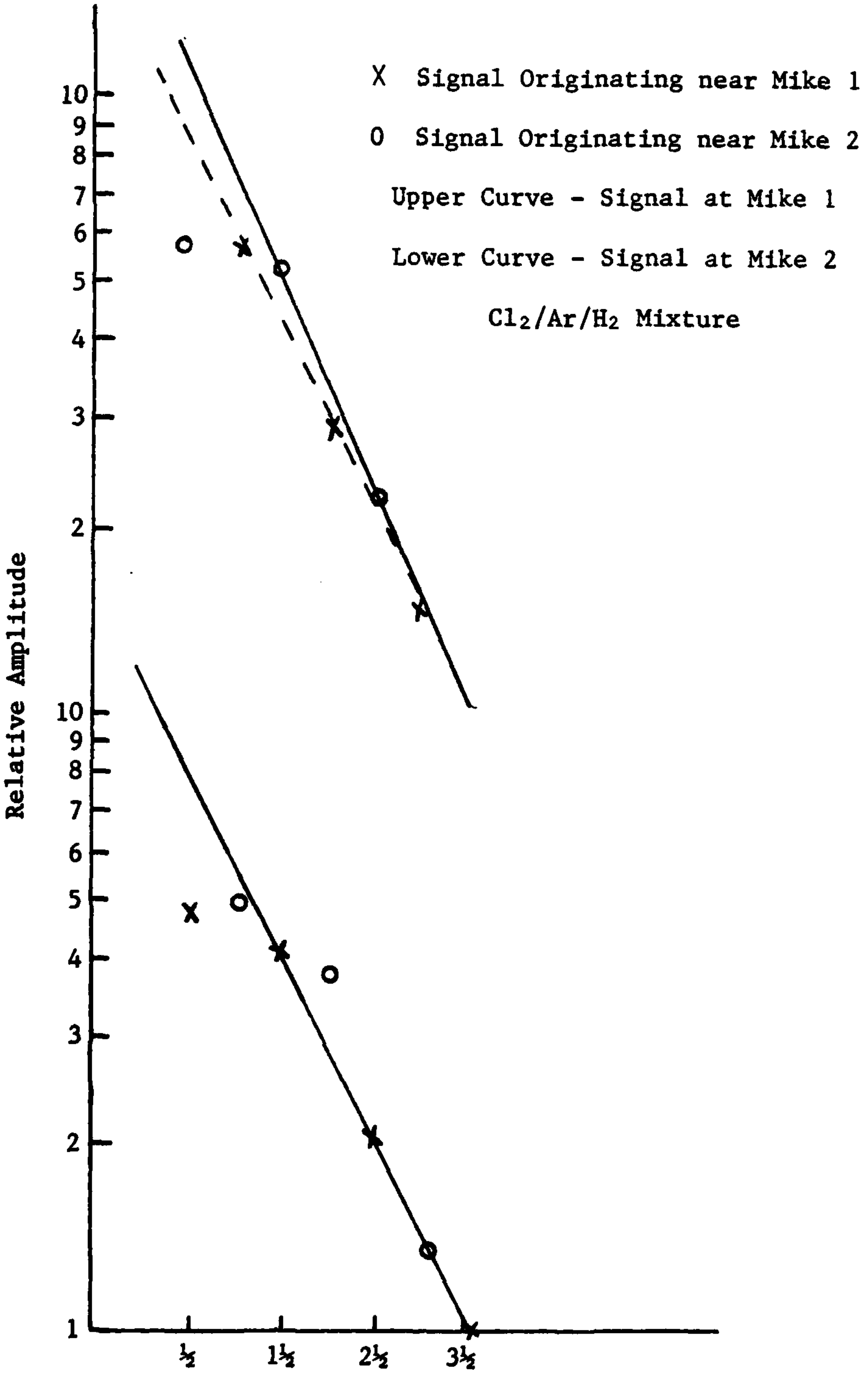

Figure 11

Signal Strength Versus Propagation Distance for 2kHz Signal extrapolating the line back to 1/2 m, we determined the effective gain which took place in the time necessary for the signal to travel this 3/4 m; the gain was 1.8 (two other sets of data give gains of 1.8 and 1.5). This means that for a propagation distance greater than 3/4 m, the signal amplitude is 1.8 times what it would have been without amplification. A gain of 4 was predicted for the mixtures used.

There are additional features of this data which serve to convince us that amplification has been observed in the pulsed system. Comparing figures (10) and (11), note that for mike 1 with H_2, B_1^2 is larger in magnitude than B_1^1; in the absence of H_2, B_1^1 is larger. The geometry was the same so the ratio of A_1^1 to A_1^2 should be the same unless B_1^2 has experienced more amplification in the 1/4 m greater distance it traveled compared to B_1^1.

Both these observations seem convincing, but, unfortunately the results are not conclusive. The large unfiltered pulse amplitude raises the possibility of non-linear effects in the gas. One would generally expect a non-linear wave to decay more rapidly leading to a curve with decreasing steepness, opposite to that seen in figure (11). But the fundamental of the pulse is at a much lower frequency so there could be a build up at higher frequencies due to steepening of pulse wave forms. The appearance of steepening is not obvious from the data, yet we are not prepared to rule out this possibility entirely.

The magnitude of the observed gains are about 1/2 that predicted by Gilbert's computer program. There are several possible explanations for this discrepancy. The computer program did not include wall collisions or expansion into the unilluminated regions (which cools the gas). Wall collisions or expansion could slow the reaction scheme. The effect of wall collisions should be small and could be explored by reproducing the experiment at lower pressures where wall collisions are more important. Cooling effects caused by the unilluminated regions were overcome in the cw-SACER experiments.

Another possible cause for the difference between observed and predicted amplification rates is the uncertainty in the UV energy supplied by the flash lamps. The energy from the flash lamps was estimated by flashing (with a given flash intensity) with different Cl_2 pressures in the tube, observing the total overpressure, then comparing this to the theory with the original Cl produced used as an adjustable variable to obtain agreement between theory and prediction. An example is given in figure (12). This technique neglects the unilluminated regions and, hence, underestimates the Cl concentration in the illuminated region. But that underestimate should not be greater than 10 percent (the volume ratio) which would not entirely explain the difference between observed and predicted gain.

cw-SACER

During cw-SACER experiments, the UV-flourescent lamps continuously dissociated Cl_2, providing atomic Cl for reactions 62 through 66. For all but one experiment, a tone burst was sent down the tube 108msec after the lamps were started; the receiving transducer monitored the tone burst as

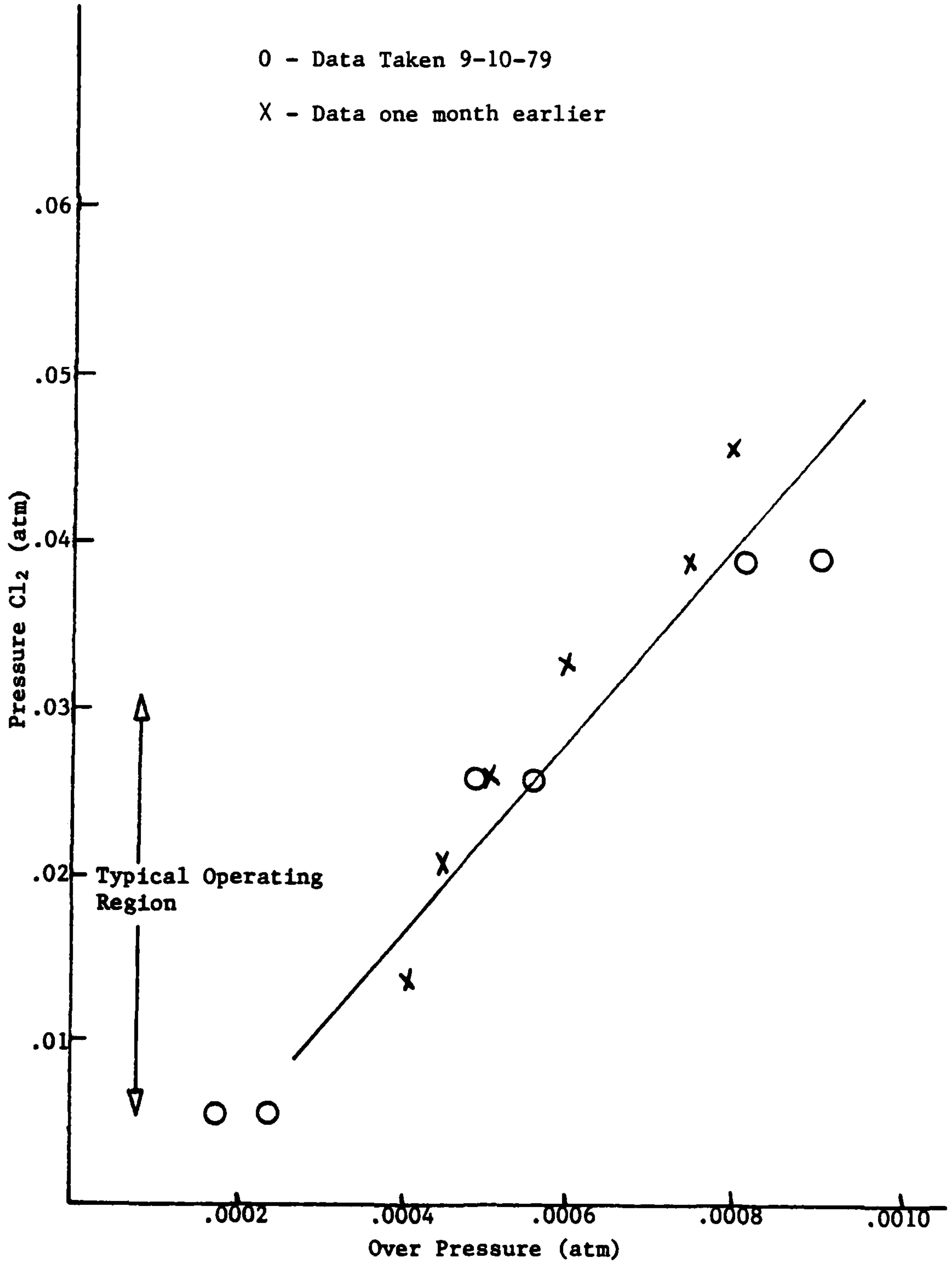

Figure 12

Cl_2 Pressure Versus Pressure Pulse 250 Joules Two Flash Lamps it propagated back and forth inside the tube. Tone bursts were also sent before and after each experiment as a control.

Experimentally, the amounts of Cl_2, H_2, and SF_6, initially in the system, could be controlled. Unlike the pulsed system, lamp intensity was not variable. Initial gas concentrations similar to those used by Toong[7] were selected for the cw-SACER experiments. Three $Cl_2:H_2:SF_6$ ratios, at a pressure of 1/3 atm, were selected, 0.5:2:17.5, 1:2:17, and 2:2:16. For each ratio, experiments were conducted for four acoustic frequencies, 1.0, 2.5, 4.0, and 6.5kHz.

For the initial conditions selected, the reactions proceeded slowly and gave predicted amplification which varied only a small amount in the time it took for a tone burst to decay to below the noise level. Therefore the tone bursts, sent while the reactions were proceeding, decayed exponentially with distance, but with a smaller attenuation coefficient than tone busts sent when the reactions were not progressing. The filtered signal from the receiving transducer was digitized and later used to obtain plots of tone burst amplitude versus distance and time (see fig. (13)).

Table (3) and fig. (14) show the data from the cw-SACER experiments just described. The plots of tone burst amplitude versus distance and time were used to obtain attenuation coefficients and velocities. In table (3), the quantities listed in the "before" columns are averages of measurements taken before and after the reactions. After the lamps were turned off and the mixture was allowed to cool, the attenuation coefficient and sound velocity were the same as before the reactions, within

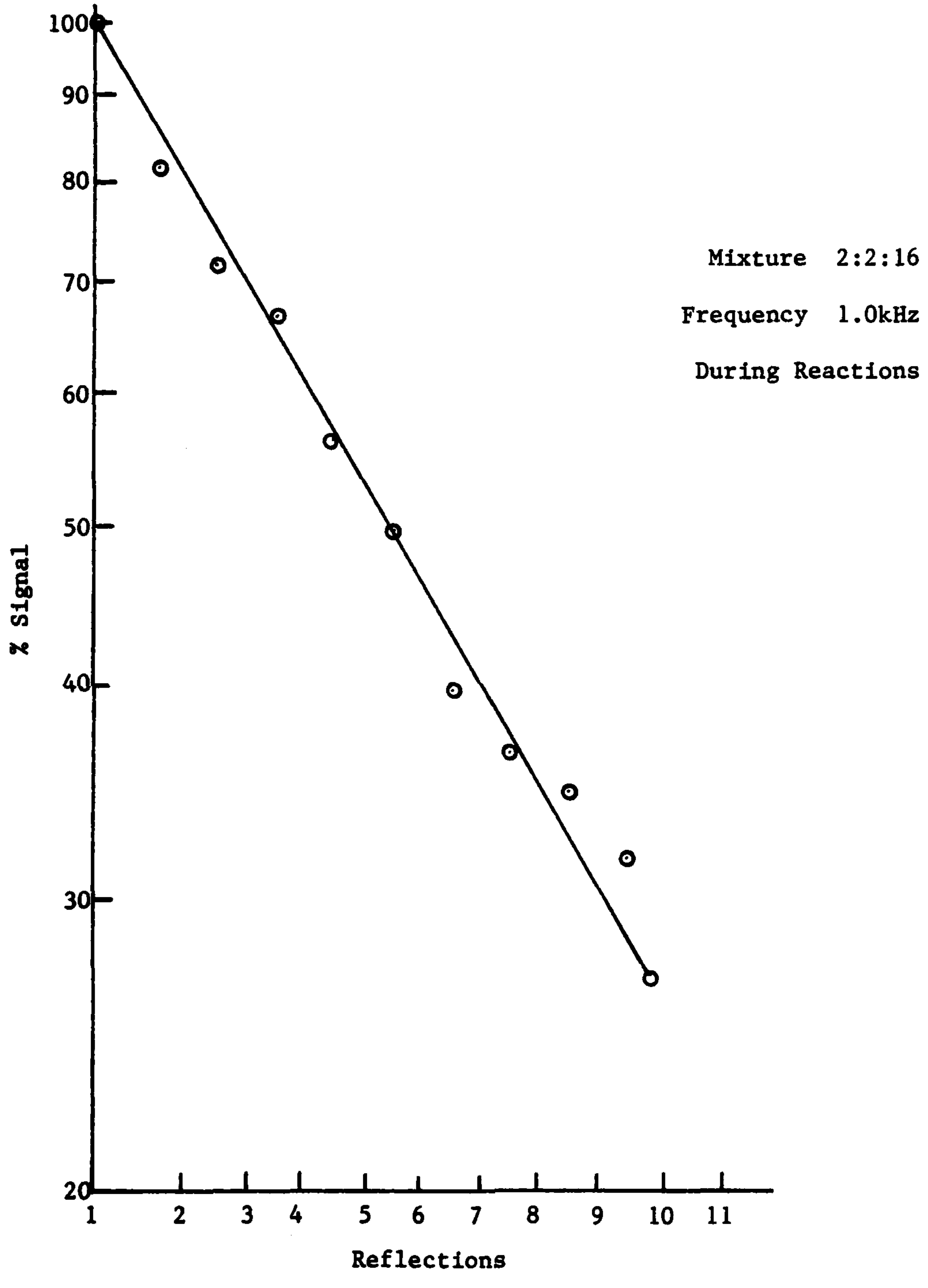

Figure 13

Pressure Amplitude Versus Propagation Distance

TABLE (3)

cw SACER Data

Frequency and Mixture H_2-Cl_2-SF_6	Attenuation (dB/cm)		$\Delta\alpha$ (dB/cm)	Velocity (m/sec)		ΔT(K)
	Before	During		Before	During	
2-2-16						
1.0 kHz	.0106	.0087	.0019	155	164	38
2.5	.0170	.0156	.0014	155	165	40
4.0	.0240	.0216	.0024	156	162	26
6.5	.0371	.0339	.0032	155	165	40
1-2-17						
1.0 kHz	.0108	.0098	.0010	152	155	14
2.5	.0177	.0162	.0015	154	156	10
4.0	.0237	.0212	.0025	151	156	22
6.5	.0357	.0329	.0028	152	156	18
0.5-2-17.5						
1.0 kHz	.0107	.0102	.0005	150	151	4
2.5	.0174	.0168	.0006	149	152	12
4.0	.0238	.0223	.0006	150	152	10
6.5	.0356	.0346	.0010	149	153	18

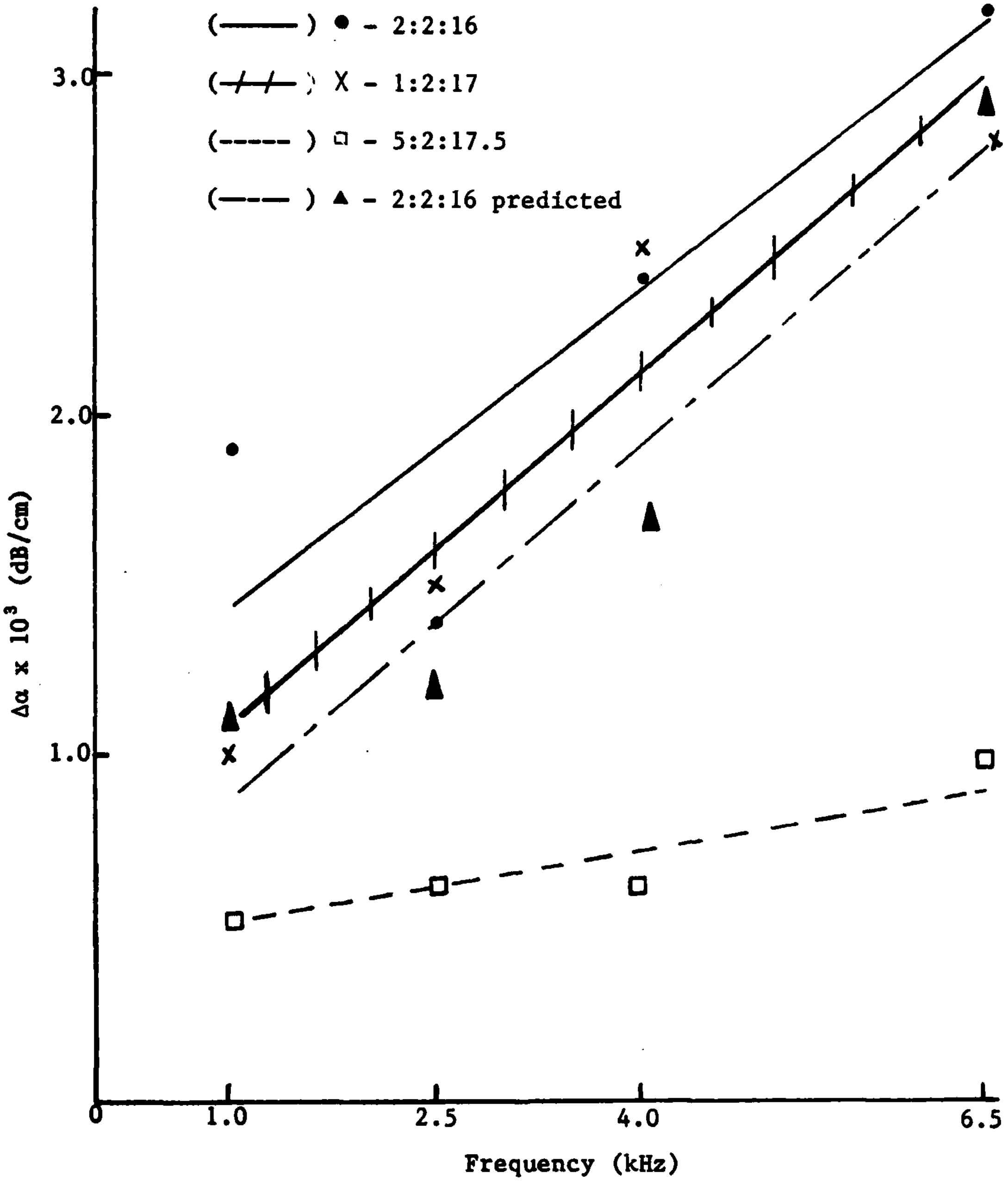

Figure 14

Δα Versus Frequency for cw-SACER Experiments experimental error. $\Delta\alpha$ is the change in attenuation while the reactions were taking place and is obtained by subtracting the "during" attenuation coefficient from the "before" attenuation coefficient. ΔT is the difference between the temperature when the reactions are progressing (determined from sound speed when the tone burst is decaying) and room temperature. ΔT is computed from the velocity measurements by using the following eq. derived from the equation for adiabatic sound velocity.

$$T_{During} = T_{Room} \left(\frac{V_{During}}{V_{Before}}\right) \tag{67}$$

The data from the 2:2:16 mixture was compared with Gilbert's computer program[6]; tube losses and classical attenuation were included in this calculation by using a slightly modified computer program originally developed by Shields[23]. The frequency factor, for reaction (62), used in the computer predictions was that value which correctly predicted the temperature change during the reactions. This frequency factor (see first assumption under eq. (49)) is related to the intensity of the fluorescent lamps. Table (4) and fig. (14) present the comparison between the predicted and observed attenuation coefficients. The observed attenuation coefficients are in fair agreement with the computer predictions. Also, the observed amplification shows the same frequency dependence as predicted.

Another cw-SACER experiment was conducted to determine the time dependence of amplification. This experiment was similar to the others except a series of tone bursts was sent; successive tone bursts were

TABLE (4)

cw-SACER Data Comparison

Mixture: 2-2-16 (H_2-Cl_2-SF_6)

Frequency (kHz)	Observed Attenuation (dB/cm)		Predicted Attenuation (dB/cm)		$\Delta\alpha$ (dB/cm)	
	Before	During	Before	During	Observed	Predicted
1.0	.0106	.0087	.0096	.0085	.0019	.0011
2.5	.0170	.0156	.0168	.0156	.0014	.0012
4.0	.0240	.0217	.0240	.0223	.0024	.0017
6.5	.0371	.0339	.0386	.0357	.0032	.0029

sent as closely spaced as possible without causing interference. A 1:2:17 ratio with a 2.5kHz tone burst was used for this experiment. Table (5) and fig. (15) present the time dependence of amplification. The point at 139msec came from a single tone burst experiment and indicates the repeatability of cw-SACER experiments. The successive tone burst experiment can be compared with an expression for $\Delta\alpha_t$ developed by Toong[7] (see eq. (55)). $\Delta\alpha_t$ is the difference between α_t before and during the reactions, where the tone burst is written as a decaying exponential, $A_0 \exp(-\alpha_t t)$. The expression for $\Delta\alpha_t$ includes the time derivative of the temperature; this derivative can be calculated only for the multiple tone burst experiment where a plot of ΔT versus time can be obtained using eq.(67). Toong's expression predicts $\Delta\alpha_t$ to be 1.13 $\sec^{-1}$ at 210msec, the observed value was 4.64 $\sec^{-1}$. Although the amplification for the single tone burst experiments cannot be easily compared with the theory developed by Toong, the frequency dependence of amplification can be compared qualitively. Fig. (14) indicates that higher frequencies are amplified more, within the frequency range studied, as predicted by Gilbert's program. However, Ref. 7 states that amplification should be independent of frequency within this range. At this time, no reason is given for the discrepancy between Toong's predictions, and our data and Gilbert's computer program.

In addition to the tone bursts, unexpected signals were sometimes observed. The signals were of two types. The first type was similar to the tone bursts, except had fewer cycles. They were approximately 70 percent as large as the tone bursts, traveled with the same velocity,

TABLE (5)

Time Dependence of cw-SACER Amplification

Mixture: 1-2-17 (H_2-Cl_2-SF_6)
Frequency: 2.5 kHz

Time(ms)	Attenuation (dB/cm)	$\Delta\alpha$ (dB/cm)
Before	0184	
53	.0169	.0015
139	------	.0015
190	.0159	.0025
315	.0127	.0057
466	.0127	.0057
735	.0146	.0038

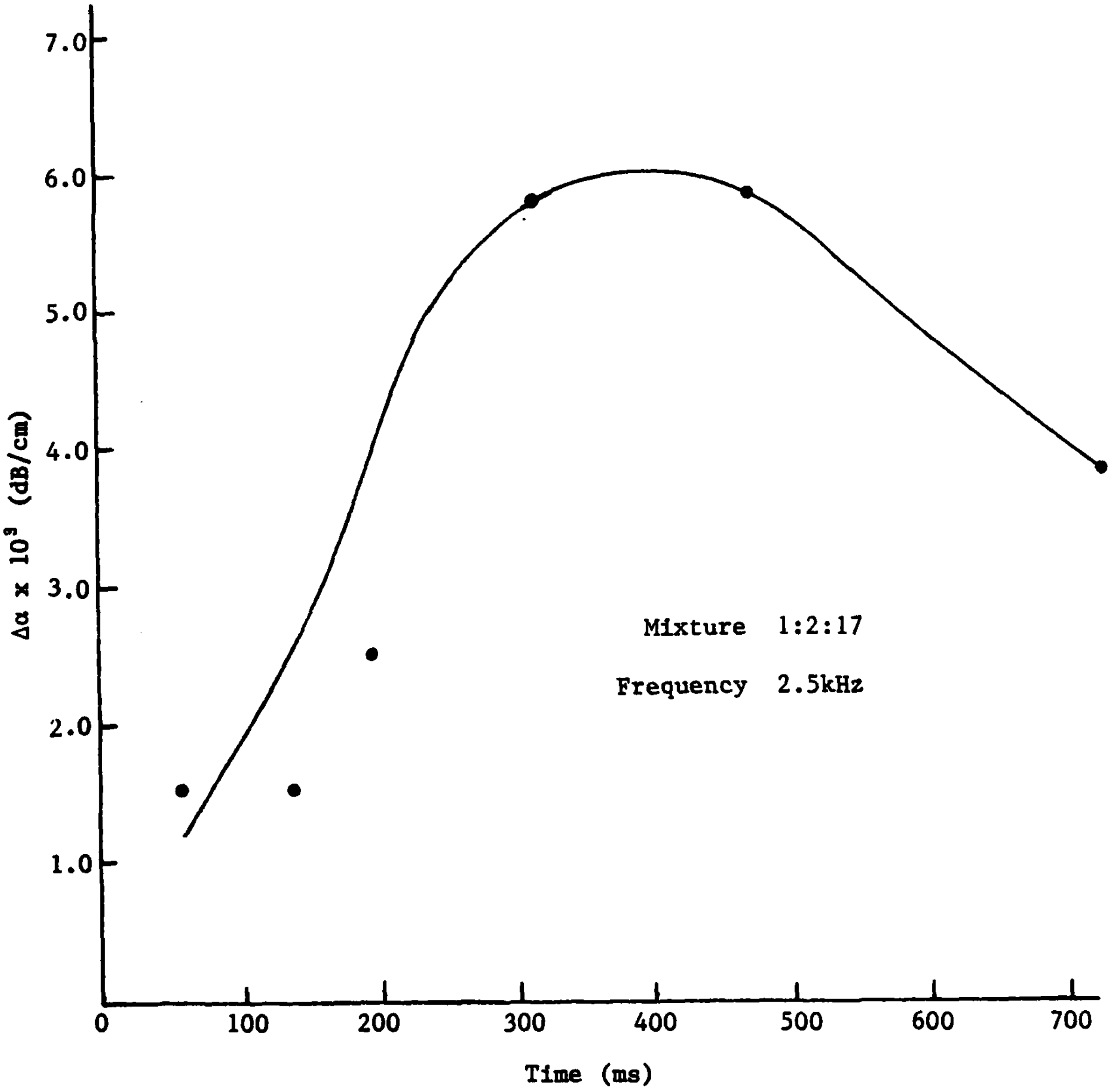

Figure 15

Δα Versus Time for cw-SACER Experiments

and sometimes decayed exponentially with the same attenuation coefficient. At first we suspected that the oscillator was being triggered by electrical noise associated with the lamps. However, the electrical noise hypothesis was later disregarded after monitoring the oscillator output while turning the lamps on.

The second type of unexpected signal appeared as a series of pulses at unpatterned intervals; each pulse was itself a series of closed spaced, positive and negative going spikes. The pulses varied in amplitude from about the same size as the tone bursts to over ten times larger; their width varied from about 1 to 1Cmsec. This type of signal was sometimes observed at low Cl_2 concentrations, but occurred frequently at higher Cl_2 concentrations. The unexpected signals made cw-SACER experiments at higher Cl_2 concentrations impossible because they completely masked the tone bursts. Repeated testing could not reproduce either type of signal without a reacting mixture in the tube. Therefore we suspect that they were both true acoustic signals. Neither type of signal has been predicted or experimentally observed before but could be the result of an instability.

Attenuation Measurements

During each attenuation experiment, a tone burst, produced by the sending transducer, was allowed to propagate back and forth in the tube while the amplitude was monitored with the receiving transducer. The amplitude of the first received tone burst was measured for different transducer separations, giving the amplitude for various propagation distances. Figure (16) shows the results of a typical attenuation experiment; the

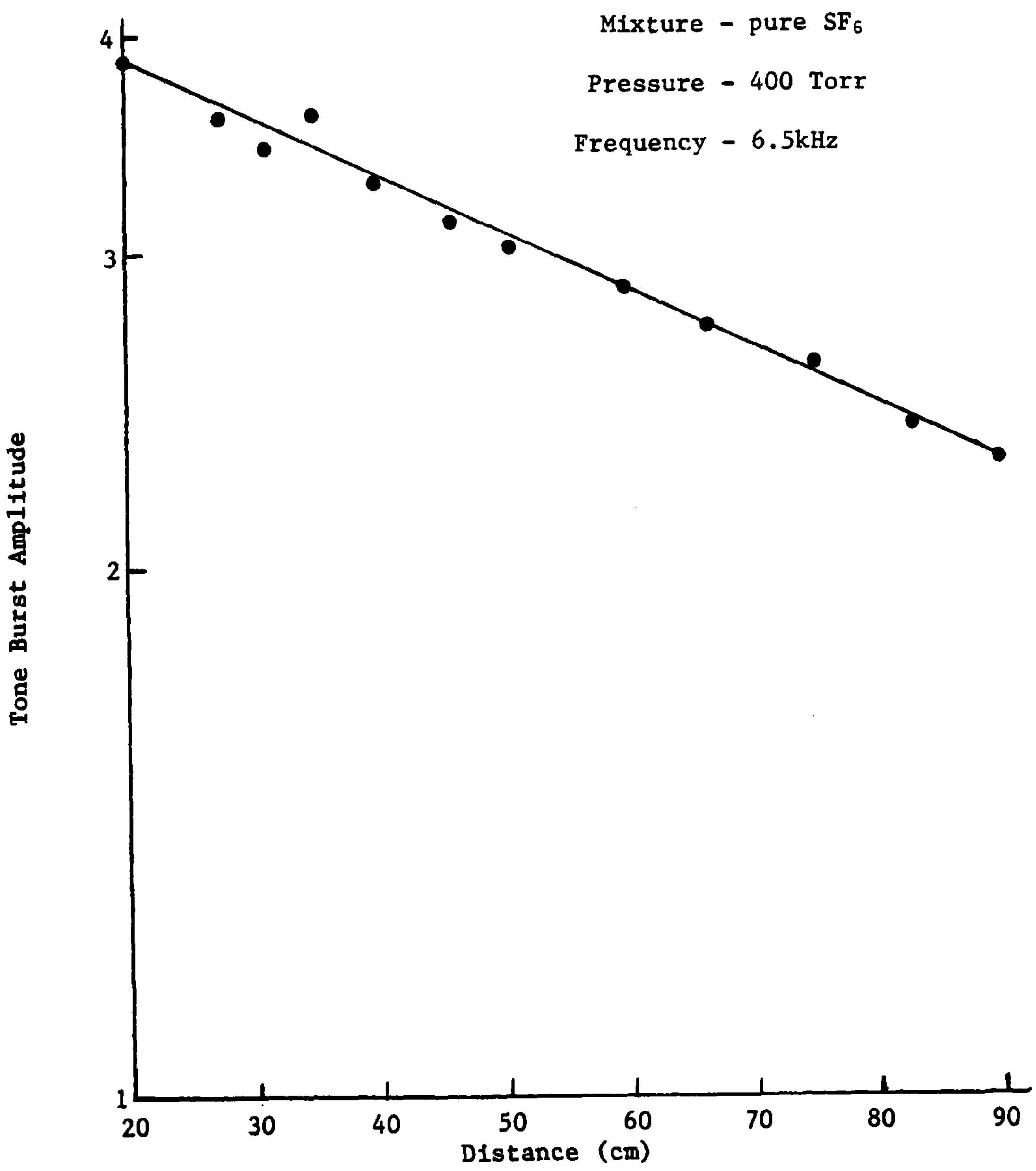

Figure 16

Pressure Amplitude Versus Propagation Distance for Attenuation Experiments

pressure amplitude is plotted, on a log scale, versus propagation distance. A straight line drawn through the points was used to calculate the attenuation.

Attenuation measurements were conducted for a number of H_2-SF_6 and Cl_2-SF_6 mixtures, and for different pressures and frequencies. Tables (6-10) show the results of these experiments.

A computer program developed by Shields[23] was used to calculate the attenuation due to vibrational relaxation by subtracting tube losses and classical attenuation from the total attenuation. The excess absorption, attributed to vibrational relaxation was used to determine vibrational relaxation times for each mixture. The log of the relaxation absorption per wavelength was plotted versus log(f/p) and the best straight line with slope 1 was used with eq. (60) to determine the quantity $(p\tau)^{-1}$ for each concentration of Cl_2 and H_2 in SF_6. Table (11) lists the vibrational relaxation times; $(p\tau)$ is pressure times the vibrational relaxation time of a given Cl_2-SF_6 or H_2-SF_6 mixture, $(p\tau)_m$ is pressure times the relaxation time for SF_6 with only collisions with m allowed, see eq. (61). For our experiments, m was either Cl_2 or H_2. $(p\tau)_m$ should be independent of the concentration of species m, but, $(p\tau)$ varies with concentration.

Additional measurements were taken to determine the reflectivity of the transducers used in the cw system. A tone burst was propagated back and forth inside the tube and monitored by the receiving transducer. The first time the tone burst reached the receiver it had propagated down the tube once; the second time the tone burst reached the receiver it had propagated down the tube three times and had been reflected twice; etc.

TABLE (6)

Attenuation Experiment # A1
Gas Mixture 100% SF_6

Pressure (Torr) / Frequency (kHz)	Attenuation (dB/cm)				
	400	200	100	50	25
2.5	.025	.030	.044	.085	.131
4	.031	.059	.094	.163	.279
6.5	.063	.119	.203	.381	.629
10	.128	.228	.401	.802	1.28
16	.301	.542	1.23	2.04	2.73
25	.808	1.51	----	4.14	5.05
35	2.00	3.18	6.79	7.96	8.27
40	----	8.56	6.48	8.26	7.73

TABLE (7)

Attenuation Experiment # AT3
Gas Mixture 20% Cl_2/80% SF_6

Pressure (Torr) / Frequency (kHz)	Attenuation (dB/cm)				
	400	200	100	50	25
2.5	.016	.028	.024	.079	.133
4	.035	.057	.096	.157	.265
6.5	.064	.105	.205	.320	.528
10	.139	.209	.368	.694	1.00
16	.319	.468	.984	1.51	2.28
25	.937	----	1.86	2.94	3.92
35	1.51	3.05	3.38	7.07	6.59
40	3.45	5.61	5.53	6.65	6.59

TABLE (8)

Attenuation Experiment # AT6
Gas Mixture 50% Cl_2/50% SF_6

Pressure (Torr) / Frequency (kHz)	Attenuation (dB/cm)				
	400	200	100	50	25
2.5	.019	.027	----	----	----
4	.05	.052	----	----	----
6.5	.06	.107	----	----	----
10	.12	.22	.35	.59	.89
16	.27	.47	----	----	----
25	.67	1.26	----	----	----
35	----	----	----	----	----
40	----	4.7	6.07	7.29	4.85
3	----	----	.048	.094	.15
5	----	----	.11	.20	.35
20	----	----	1.74	2.07	2.43
50	----	----	6.98	7.29	4.85

TABLE (9)

Attenuation Experiment # AT4
Gas Mixture 10% H_2/90% SF_6

Pressure (Torr) / Frequency (kHz)	Attenuation (dB/cm)				
	400	200	100	50	25
2.5	.011	.011	.034	.061	.064
4	.024	.034	.047	.077	.107
6.5	.020	.046	.076	.124	.197
10	.026	.071	.124	.222	.364
16	.058	.137	.251	.440	1.51
25	.142	.272	.535	2.29	1.56
35	.281	.478	1.26	2.09	4.00
40	.368	.725	1.60	3.48	3.81

TABLE (10)

Attenuation Experiment # AT5
Gas Mixture 20% H_2/80% SF_6

Pressure (Torr) / Frequency (kHz)	Attenuation (dB/cm)				
	400	200	100	25	50
2.5	.021	.017	.033	.074	.041
4	.019	.028	.035	.097	.060
6.5	.022	.033	.058	.158	.092
10	.033	.051	.095	.270	.158
16	.061	.101	.171	.550	.311
25	.138	.223	.340	3.05	.635
35	.202	.364	.594	3.06	1.11
40	.249	.390	.692	3.48	2.35

TABLE (11)

Vibrational Relaxation Values For SF_6, SF_6-H_2, and SF_6-Cl_2

SF_6 Mixture	$(p\tau)^{-1}$x10^{-6} $sec^{-1}\cdot atm^{-1}$	$(p\tau)_m^{-1}$x10^{-6} $sec^{-1}\cdot atm^{-1}$	Average $(p\tau)_m$ x10^7 sec·atm
pure SF_6	1.38 ± .24	1.38 ± 2.4	7.25
20%Cl_2	1.55 ± .34	2.25 ± .35	4.39
50%Cl_2	1.85 ± .30	2.30 ± .34	
10%H_2	7.25 ± 2.4	59.9 ± 24	0.179
20%H_2	11.5 ± 3.9	52.1 ± 20	

Inside the tube, the tone burst amplitude is given by $A_0 \exp(-\alpha x - n\beta)$ where n is the number of reflections the tone burst had undergone and β is the reflection coefficient. Using a single transducer separation and a mixture with known attenuation, the reflectivity, $\exp(-\beta)$ was calculated for three pressures of pure SF_6; 400, 200, and 100 torr (the frequency used was 4kHz). For each pressure, the reflectivity was found to be 1.0 within experimental error (less than 1 percent). Therefore, attenuation caused by reflections was not included in absorption calculations for cw-SACER experiments.

CHAPTER V

CONCLUSIONS AND SUMMARY

An experimental investigation undertaken to observe sound amplification in a chemically reacting Cl_2-H_2-inert gas has been described. A pulsed SACER was constructed for preliminary study. Intense flash lamps initiated the reactions which resulted in sound amplification for about 10msec. A gain of 1.8 at 2.5kHz was observed compared with a gain of 4 predicted by theory. This discrepancy has not been fully explained although it may have been caused by an error in predicting the flash lamp intensity.

Following the preliminary investigation, a more thorough study was undertaken. This study included a broader range of frequencies and initial conditions. During these experiments, low intensity fluorescent lamps continuously dissociated molecular chlorine; the reactions progressed for a longer time, resulting in observed amplification for over 800msec. The fluorescent lamps were more controllable than the flash lamps, so more physical parameters could be varied; this made it possible to note trends in the amplification data.

For the cw-SACER experiments, amplification increased with frequency, the values at 6.5kHz were about 2.5 times larger than the values at 1.0kHz. This agrees with predictions obtained with Gilbert's numerical solution[6], however, Toong[7] states that amplification should be independent of frequency within the range studied. The observed values for $\Delta\alpha$

were about 20 percent larger than Gilbert's program predicted, but this difference might be explained by inaccurate determination of lamp intensity. Toong has derived an expression for $\Delta\alpha_t$[7], the change in the attenuation coefficient related to exponential decay with time, which predicts an amplification only 25 percent as large as was observed. It is obvious that the assumptions on which that derivation is based are not fulfilled by this experiment.

A cw experiment was conducted which observed the time dependence of amplification. 'For the conditions chosen (Cl_2:H_2:SF_6 ratio of 1:2:17 at 1/3atm and a frequency of 2.5kHz) amplification increased rapidly for the first 300msec, peaked at about 400msec, then started to decrease. The temperature of the mixture followed a similar curve. As the gas heats up most of the reaction rates increase, so it is not surprising that amplification increases. A point is probably reached where the supply of atomic H becomes depleted and reaction (64), a very exothermic reaction, slows down to the point where more heat is lost through the tube walls than is generated by the reactions.

For the cw experiments in which only one tone burst was sent down the tube, amplification increased with Cl_2 concentration. This is expected because increasing the Cl_2 concentration also increased the amount of atomic Cl available for reactions (64) through (65).

Two types of unexplained signals were observed during the cw experiments. Both appear to be real since they could not be duplicated without a reacting mixture in the tube. The first type was similar in amplitude to the tone bursts, traveled with the same speed, and sometimes decayed exponentially with the same attenuation coefficient. The second type was much larger than the tone bursts and did not propagate back and forth the tube. The second type was observed frequently when the Cl_2 concentration was large or when the temperature was high.

It is clear that future studies of amplification in reacting systems is merited. Both of our studies were hampered by the question of light intensity within the tube. Perhaps a fiber optics probe could be used to determine light intensity within the tube. Some measurements have been made in our lab with a fiber optic probe positioned outside the tube, but with little success. Two types of unexplained signals were observed during the cw experiments. Since neither signal was theoretically predicted, a set of experiments should be conducted to determine their origin. A type of chemical instability may be responsible. A final suggestion for further study is to develop a system with flowing gases so that the reactants are continuously renewed. Such a system would allow signal averaging and thus lessen experimental error.

REFERENCES

1. T.Y. Toong, P. Arbeau, C.A. Garris, and J.P. Patureau, Symposium (International) on Combustion, 15th, The Combustion Institute, 87, 1975.

2. A. Einstein, S.B. preuss. Akad. Wiss., 18, 1920.

3. B.T. Chu, Proceedings of Heat Transfer and Fluid Mechanics Institute (Stanford University Press, 1958).

4. J.F. Clark and M. McChesney, The Dynamics of Real Gases (Butterworths, 1964).

5. R.J. Ellis and R.G. Gilbert, J. Acoust. Soc. Am. 62 (2), 245, 1977.

6. S.A. Edwards, R.J. Ellis, and R.G. Gilbert, Sound-In-Gas-Phase-Reactions (computer program, personal communication, 1975).

7. G.E. Abouseif, T. Toong, and J. Converti, Symposium (International) on Combustion, 17th, University of Leeds, 1341, 1978.

8. J.P. Patureau, T.Y. Toong, and C.A. Garris, Symposium (International) on Combustion, 16th, The Combustion Institute, 929, 1977.

9. T.Y. Toong, P. Arbeau, C.A. Garris, and J.P. Patureau, Symposium (International) on Combustion, 15th, The Combustion Institute, 87, 1975.

10. R. Tal, J. Sound Vib., 80 (1), 97, 1982.

11. J.P. Platureau, Acoustic-Kinetic Interactions in Non-Equilibrium H_2-Cl_2 Reactions, Sc.D. Thesis, Massachusetts Institute of Technology, 1976.

12. R.G. Gilbert, H. Hahn, P.J. Ortoleva, and J. Ross, J. Chem. Phys., 57, 2672, 1971.

13. R. G. Gilbert, P. Ortoleva, and J. Ross, J. Chem. Phys., 58, 3625, 1973.

14. U. Ingard and M. Schulz, Phys. Fluids, 11, 688, 1968.

15. E.P. DePlomb, Phys. Fluids, 14, 448, 1971.

16. H.J. Bauer and H.E. Bass, Phys. Fluids, 16, 988, 1973.

17. F.D. Shields, Dept. of Phys., University of Mississippi, personal communication.

18. D.D. Fitts, Nonequilibrium Thermodynamics (McGraw-Hill, New York, 1962).

19. C.W. Gear, Numerical Initial Value Problems in Ordinary Differential Equations (Prentice-Hall, New York, 1971).

20. L.E. Kinsler and A.R. Frey, Fundamentals of Acoustics, second edition (John Wiley & Sons, New York, 1962).

21. J.W. Strutt Lord Rayleigh, Theory of Sound, second edition (Dover Publications, New York, 1945).

22. P.S. Henry, Proc. Phys. Soc. (London) 43, 340, 1931.

23. F.D. Shields and J. Faughn, J. Acoust. Soc. Amer. 46 (1), 158, 1969.

24. F.D. Shields, K.P. Lee and W.J. Wiley, J. Acoust. Soc. Amer. 37, 724, 1965.

25. F.D. Shields, Dept. of Phys., University of Mississippi, personal communication.

26. P.M. Morse and K.U. Ingard, Theoretical Acoustics (McGraw-Hill, 1968).

27. H.E. Bass, L.C. Sutherland, J. Piercy, and L. Evans (to be published in Physical Acoustics, Academic Press, New York).

28. H.J. Bauer, F.D. Shields, and H.E. Bass, J. Chem. Phys. 57 (11), 4624, 1972.

29. H.E. Bass, Final Report on an Experimental Study of Vibrational Relaxation of UF_6, WF_6, and MoF_6 (University of Mississippi, 1982).

APPENDIX A

COMPUTER PROGRAMS USED TO PREDICT AMPLIFICATION

Program RICABS.F4

This program was used with Gilbert's computer program[6] to predict sound amplitude for cw-SACER experiments. A similar program was used for the pulsed SACER predictions.

```
      IMPLICIT REAL*8 (A-H,O-Z)
      DIMENSION XY(3),PHD(3,3),WZ(3),VVIS(3)
        DIMENSION ARX(3),AIX(3),BF0R(3),BF0I(3)
        DIMENSION PBR(3),PBI(3),BF1R(3),BF1I(3),UT(6)
        DIMENSION TY(30)
CC
        DIMENSION Y(79),Y11(79),Y12(79),Y13(79),Y22(79)
CCC
      SQRTF(X)=DSQRT(X)
      COSF(X)=DCOS(X)
      SINF(X)=DSIN(X)
      EXPF(X)=DEXP(X)
CC
        N=79
        DO 400 J=1,N
      READ(10,410) Y(J),Y11(J),Y12(J),Y13(J),Y22(J)
  400 CONTINUE
  410 FORMAT(5F)
CCC
1     FORMAT(5D/4D)
2     FORMAT(2D)
100   FORMAT(6H  E1V=D13.6,1X6H  E1A=D13.6)
102   FORMAT(4H  T=D12.5,1X4H  W=D12.5,1X5H  C8=D12.5,1X5H  CV=D13.6)
103   FORMAT(7H  VIS =D12.5,7H P(MM)=D12.5,7H R(CM)=D12.5,4H FM=D12.5)
104   FORMAT(7H TA+CA=D12.5,4H RA=D12.5,1X6HWL(M)=D12.5,5H FSV=D12.5)
105   FORMAT(6H  ACS=D12.4,6H  ACT=D12.4,3X,'SRTMG=',D12.5,//)
106   FORMAT(5H RAP=D12.5,6H FSVP=D12.5,1X6HALFAP=D12.5,6H VELP=D12.5)
107   FORMAT(4H RW=D12.5,5H  RP=D12.5,7H GAMAR=D12.5,7H GAMAI=D13.6)
108     FORMAT(1X,'F=',F5.1,2X,'MS=',D9.3,2X,'V=',D10.4,
     *2X,'V(%)=',F4.0,2X,'V/W=',D10.3,' /',F6.0,/)
        W1=146.
        W2=71.0
        W3=2.0
        R=1.23
C       R=1.27
        ACS=1.
        ACT=1.
CC
        SM1=5.51
        SM2=4.40
                SM3=2.9
       EOK3=37.
        EOK1=200.9
        EOK2=257.0
        SM12=(SM1+SM2)/2.
       SM23=(SM2+SM3)/2.
       SM13=(SM1+SM3)/2.
        EOK12=(EOK1*EOK2)**0.5
       EOK23=(EOK2*EOK3)**0.5
       EOK13=(EOK1*EOK3)**0.5
        TABS=0.
        TDL=0.
        READ(7,665) FREQ
        F=FREQ/(2.*3.1416)/1000.
        WRITE(8,880) F
  880 FORMAT(2X,'FREQ=',F10.2,2X,'KHZ.',/)
        WRITE(8,890)
  890 FORMAT(3X,'TIME',6X'TEMP',4X,'P(ATM)',2X'AMP',4X,'NEWAMP',
     12X'TOTALABS',2X'DIST',5X'DB/M',/)
 665    FORMAT(9D)
```

```
        CV1=3.0
        CV2=2.5
        CV3=2.5
        C81=1.5
        C82=1.5
        C83=1.5
        READ(7,665) TIME,TEMP,PATM,AMP,FM1,FM2,FM3
        AMPNEW=AMP
        WRITE(8,800) TIME,TEMP,PATM,AMP,AMPNEW,TABS
  800 FORMAT(1X,F8.5,F9.2,3F8.3,4F9.5)
 600    CONTINUE
        OTIME=TIME
        READ(7,665,END=99) TIME,TEMP,PATM,AMP,FM1,FM2,FM3
        P=760.*PATM
        T=TEMP
        TS1=T/EOK1
        TS2=T/EOK2
       TS3=T/EOK3
       TS23=T/EOK23
       TS13=T/EOK13
        TS12=T/EOK12
        CALL SSEVAL(N,TS12,Y,Y11,SEVAL)
        OM11=SEVAL
        CALL SSEVAL(N,TS12,Y,Y12,SEVAL)
        OM12=SEVAL
        CALL SSEVAL(N,TS12,Y,Y13,SEVAL)
        OM13=SEVAL
        CALL SSEVAL(N,TS12,Y,Y22,SEVAL)
        OM22=SEVAL
        CALL SSEVAL(N,TS1,Y,Y22,SEVAL)
        OM221=SEVAL
        CALL SSEVAL(N,TS2,Y,Y22,SEVAL)
        OM222=SEVAL
      CALL PD(W1,W2,TEMP,SM12,OM11,PRD(1,2),PRD(2,1))
C         TYPE 927,PRD(1,2)
927          FORMAT(2X,'PRD(1,2)=',D12.5)
       VVIS(1)=266.93*10**-7.*(W1*T)**0.5/(SM1*SM1*OM221)
        VVIS(2)=266.93*10**-7.*(W2*T)**0.5/(SM2*SM2*OM222)
C          TYPE 937,VVIS(2)
937          FORMAT(2X,'VVIS(2)=',D12.5)
C*      TYPE 402,TS1,TS2,TS12,OM11,OM221,OM222
  402 FORMAT(2X,6F9.3)
CC
        FM2=1.-FM1-FM3
        XX=(FM1/W1)+(FM2/W2)+(FM3/W3)
        X1=FM1/W1/XX
        X2=FM2/W2/XX
        X3=FM3/W3/XX
        W=X1*W1+X2*W2+X3*W3
C       TYPE 947,X1,X2,X3,FM1,FM2,FM3
947     FORMAT(2X,6(2X,D12.5))
        CV=X1*CV1+X2*CV2+X3*CV3
        C8=X1*C81+X2*C82+X3*C83
        CALL SSEVAL (N,TS23,Y,Y11,SEVAL)
        OM11=SEVAL
        CALL SSEVAL(N,TS23,Y,Y12,SEVAL)
        OM12=SEVAL
        CALL SSEVAL(N,TS23,Y,Y13,SEVAL)
        OM13=SEVAL
        CALL SSEVAL(N,TS23,Y,Y22,SEVAL)
```

```
        OM22=SEVAL
        CALL SSEVAL(N,TS2,Y,Y22,SEVAL)
        OM221=SEVAL
        CALL SSEVAL(N,TS3,Y,Y22,SEVAL)
        OM222=SEVAL
      CALL PD(W2,w3,TEMP,SM23,OM11,PRD(2,3),PRD(3,2))
       VVIS(3)=266.93*10**-7.*(W3*T)**0.5/(SM3*SM3*OM222)
        CALL SSEVAL(N,TS13,Y,Y11,SEVAL)
        OM11=SEVAL
        CALL SSEVAL(N,TS13,Y,Y12,SEVAL)
        OM12=SEVAL
        CALL SSEVAL(N,TS13,Y,Y13,SEVAL)
        OM13=SEVAL
        CALL SSEVAL(N,TS13,Y,Y22,SEVAL)
        OM22=SEVAL
        CALL SSEVAL(N,TS1,Y,Y22,SEVAL)
        OM221=SEVAL
        CALL SSEVAL(N,TS3,Y,Y22,SEVAL)
        OM222=SEVAL
       CALL PD(w1,W3,TEMP,SM13,OM11,PRD(1,3),PRD(3,1))
C       CACULATION OF VISCOSITY FOR 3 GASES USING
C       DIFFUSION CONSTANTS FOR TWO GASES
       XY(1)=X1
       XY(2)=X2
       XY(3)=X3
       WZ(1)=w1
       WZ(2)=w2
       WZ(3)=w3
       VIS=0.
       DO 990 I=1,3
       PPD=0
       DO 980 K=1,3
       IF(K.EQ.I) GO TO 980
       PPD=PPD + (1.385*XY(I)*XY(K)*8.3144D3/(PRD(I,K)*WZ(I)))
917      FORMAT(4D12.5)
C       TYPE 933,PPD
C       TYPE 917,XY(I),XY(K),PRD(I,K),WZ(I)
980    CONTINUE
        IF(XY(I).LT.1D-5)GO TO 990
       VIS=VIS + (XY(I)**2./(XY(I)**2./VVIS(I)+PPD))
C       TYPE 913,VIS,VVIS(I),PPD
913     FORMAT(2X,'VIS=',D12.5,'VVIS=',D12.5,'PPD=',D12.5)
990    CONTINUE
C           TYPE 933,PPD
933         FORMAT(2X,'PPD=',D12.5)
C           TYPE 939,VIS
939                    FORMAT(2X,'VIS=',D12.5)
80      CONTINUE
        V=VIS
        RTM=8.3144D7*T/W
        ZROT=63.3/EXP(16.7/T**.333333)
        FM=(2.5+1.)*1.25*1014000./V/ZROT/(6.2832*2.5)/1.
        SRTMG=SQRTF(RTM*(1.D0+1.D0/CV))
CK      WRITE(3,102)T,W,C8,CV
CK      WRITE(3,103)V,P,R,FM
CK      WRITE(3,105) ACS,ACT,SRTMG
      AF=2.D0*3.1416D0*1000.D0*F
      AT=F*760.D0*SQRTF(CV*(CV+1.D0)/(C8*(C8+1.D0)))/(FM*P)
C       TYPE 973,FM
973     FORMAT(2X,'FM=',D12.5)
```

```
         WL=SRTMG/(F*1000.)/100.
      PDN=1.3332D3*F
         RTM=8.3144D7*T/W
      VUD=V*RTM/PDN
         C1=X1*1.5+X2*1.0+X3*1.0
         C2=7.692
         AT1=AT
         PTSF6=7.25E-7
         PTCL2=4.37E-7
        PTH2=1.78E-8
         PTMIX=1./(X1/PTSF6+X2/PTCL2+X3/PTH2)
         AT2=760./P*PTMIX
C        AT1=1.0E-9
C        AT2=1.0E-9
C        TYPE 967,AT1,AT2
967      FORMAT(2X,'AT1=',D12.5,2X,'AT2=',D12.5)
         AF2=AF*AF
         PA1=1.+AT1*AT1
         PA2=1.+AF2*AT2*AT2
         C1=CV-C8
         C2=X1*C2
      A2=CV*CV+C8*C8*AT*AT
         CVR=C8+C1/PA1+C2/PA2
         CVI=-(C1*AF*AT1/PA1+C2*AF*AT2/PA2)
         CVAV2=CVR*CVR+CVI*CVI
      URN=VUD*(1.D0+2.25D0*CVR/CVAV2)
      UIN=-2.25D0*CVI/CVAV2*VOD
         RSHR=1.D0+CVR/CVAV2
         RSHI=-CVI/CVAV2
         BR=-RTM*RSHR+AF*UIN
         BI=-RTM*RSHI-AF*(URN+1.33333D0*VOD)
      AR=1.3333D0*VUD*URN+RTM*UIN/AF
      AI=1.3333D0*VOD*UIN-RTM*URN/AF
      AB=2.D0*(AR*AR+AI*AI)
      ABR=-(BR*AR+BI*AI)/AB
      ABI=-(BI*AR-BR*AI)/AB
      ARAR=AR*AR+AI*AI
      FR=ABR*ABR-ABI*ABI+AF*AF*AR/ARAR
      FI=2.D0*ABR*ABI-AF*AF*AI/ARAR
      FRI=SQRTF(FR*FR+FI*FI)
      IF(FI) 11,12,12
11    GR=SQRTF(-(FRI+FR)/2.D0)
      GO TO 13
12    GR=SQRTF((FRI+FR)/2.D0)
13    GI=SQRTF((FRI-FR)/2.0D0)
      RL2=ABR+GR
      FI2=ABI+GI
      RL1=ABR-GR
      FI1=ABI-GI
      ATM=P/760.D0
      RF=SRTMG/AF
      RFS=RF*RF
      G1SR=RL1*RFS
      G1SI=FI1*RFS
      G2SR=RL2*RFS
      G2SI=FI2*RFS
      RF=R/RF
C*       TYPE 501,G1SR,G1SI
C*       TYPE 501,G2SR,G2SI
501   FORMAT(5D/4D)
```

```
      RW=SRTMG*SRTMG/(VOD*AF)
      SQIGR=URN/VOD
      SQIGI=UIN/VOD
      G1SAV=G1SR*G1SR+G1SI*G1SI
      BET1R=G1SI/G1SAV-SQIGR/RW
      BET1I=G1SR/G1SAV-SQIGI/RW
      G2SAV=G2SR*G2SR+G2SI*G2SI
      BET2R=G2SI/G2SAV-SQIGR/RW
      BET2I=G2SR/G2SAV-SQIGI/RW
      FKPA=F/ATM
      FN=FKPA/FM
      GZERO=1.D0+(1.D0/CV)
      GINF=1.D0+(1.D0/C8)
      CG=GZERO*(1.D0+FN*FN)/(1.D0+(GZERO*FN*FN/GINF))
      TC=(CG-1.D0)/CG
      TB=(9.D0*CG-5.D0)/4.D0
      TK=13.3339D0*(1.D0/SQRTF(CG)+TC*SQRTF(TB))*SQRTF(V)/R
      TA=TK*SQRTF(F/P)
      FSV=SQRTF(8.3144D3*CG*T/W)
C       TYPE 940,FSV
940     FORMAT(5F)
      DELV=TK*FSV*FSV*.0018323D0/SQRTF(F*P)
      CA=(1.333333D0+TC*TB)*V*SQRTF(W/T)
      CA=14.106D0*CA*F*F/(P*SQRTF(CG*CG*CG))
      RA=3141.62D0*(CV-C8)/SQRTF((CV+1.D0)*(C8+1.D0)*CV*C8)
      VEL=(FSV-DELV)*100.D0
C       TYPE 940,VEL
      TV=VEL
      RA=RA*FN*F/(VEL*(1.D0+FN*FN))
      ALPHA=RA+(TA+CA)/8.686D0
      TCA=(TA+CA)*100.
      ALFA=ALPHA
      PCR=+ALPHA
      PCI=AF/VEL
      PC2R=PCR*PCR-PCI*PCI
      PC2I=2.D0*PCR*PCI
C*      WRITE(3,104) TCA,RA,WL,FSV
7     Z1I=PC2I-AF/VOD
      ARAR=SQRTF(PC2R*PC2R+Z1I*Z1I)
      AR1R=-R*SQRTF((PC2R+ARAR)*.5D0)
      AR1I=R*SQRTF((-PC2R+ARAR)*.5D0)
      Z3R=PC2R-RL2
      Z3I=PC2I-FI2
      ARAR=SQRTF(Z3R*Z3R+Z3I*Z3I)
      AR3R=-R*SQRTF(.5D0*(ARAR+Z3R))
      AR3I=R*SQRTF(.5D0*(ARAR-Z3R))
      Z2R=PC2R-RL1
      Z2I=PC2I-FI1
      ARAR=SQRTF(Z2R*Z2R+Z2I*Z2I)
      AR2R=R*SQRTF(.5D0*(ARAR+Z2R))
      AR2I=R*SQRTF(.5D0*(ARAR-Z2R))
      ARX(1)= AR1R
      ARX(2)= AR2R
      ARX(3)=AR3R
      AIX(1)= AR1I
      AIX(2)= AR2I
      AIX(3)=AR3I
      DO 30 J=1,3
      AR= ARX(J)
      AI= AIX(J)
```

```
      AA=SQRTF(AR*AR+AI*AI)
      IF(AA-6.)19,19,25
19    COSX=AR/AA
      SINX=AI/AA
      COS2X=1.D0-2.D0*SINX*SINX
      SIN2X=2.D0*COSX*SINX
      B1I=AA*SINX/2.D0
      B1R=AA*COSX/2.D0
      F1M=AA/2.D0
      DO 20 I=1,30
      X=I
      COSPX=COSX
      COSX=COSX*COS2X-SINX*SIN2X
      SINX=SINX*COS2X+COSPX*SIN2X
      F1M=-F1M*AA*AA/(4.D0*X*(X+1.D0))
      B11R=COSX*F1M
      B1R=B1R+B11R
      B11I=SINX*F1M
      B1I=B1I+B11I
      IF(F1M*F1M-.00000001)21,21,20
20    CONTINUE
21    COSX=AR/AA
      SINX=AI/AA
      COS2X=1.D0-2.D0*SINX*SINX
      SIN2X=2.D0*COSX*SINX
      COSX=COS2X
      SINX=SIN2X
      F0M=-AA*AA/4.D0
      B0R=1.D0-AA*AA*COSX/4.D0
      B0I=-AA*AA*SINX/4.D0
      DO 22 I=2,30
      X=I
      F0M=-F0M*AA*AA/(4.D0*X*X)
      COSXP=COSX
      COSX=COSX*COS2X-SINX*SIN2X
      SINX=SINX*COS2X+COSXP*SIN2X
      B01R=F0M*COSX
      B01I=F0M*SINX
      B0R=B0R+B01R
      B0I=B0I+B01I
      IF(F0M*F0M-.00000001)23,22,22
22    CONTINUE
23    GO TO 26
25    AR=-AR
      AI=-AI
      SRZR=SQRTF(.5D0*(AA+AR))
      SRZI=-SQRTF(.5D0*(AA-AR))
 18     AA2=AA*AA
        AA3=AA2*AA
        AA4=AA2*AA2
        AA5=AA4*AA
        AA6=AA4*AA2
      C1R=.7978846D0*SRZR/AA
      C1I=-.7978846D0*SRZI/AA
      ARSR=AR*AR-AI*AI
        ARSR=ARSR/AA2
      ARSI=2.D0*AR*AI
        ARSI=ARSI/AA2
      ARCR=AR*ARSR-AI*ARSI
        ARCR=ARCR/AA
```

```
      ARCI=AI*ARSR+AR*ARSI
        ARCI=ARCI/AA
      ARFR=ARSR*ARSR-ARSI*ARSI
        ARFR=ARFR/AA
      ARFI=2.D0*ARSR*ARSI
        ARFI=ARFI/AA
      ARPR=ARFR*AR-ARFI*AI
        ARPR=ARPR/AA
      ARPI=ARFR*AI+ARFI*AR
        ARPI=ARPI/AA
      ARHR=ARCR*ARCR-ARCI*ARCI
        ARHR=ARHR/AA
      ARHI=2.D0*ARCR*ARCI
        ARHI=ARHI/AA
      CBR1=1.D0+.117188D0*ARSR/AA2-.14420D0*ARFR/AA4
      CBR1=CBR1+.67659279D0*ARHR/AA6
      CBI1=-.117188D0*ARSI/AA2+.14420D0*ARFI/AA4
      CBI1=CBI1-.67659279D0*ARHI/AA6
      SBR1=.375D0*AR/AA2-.10254D0*ARCR/AA3+.27758D0*ARPR/AA5
      SBI1=-.375D0*AI/AA2+.10254D0*ARCI/AA3-.27758D0*ARPI/AA5
      A1=COSF(AR-2.356195D0)
      A2=SINF(AR-2.356195D0)
        IF(AI.LT.40.) GO TO 201
        EP=1.0D0
        EN=0.0D0
201     IF(AI.GT.-40.) GO TO 202
        EP=0.0D0
        EN=1.0D0
        GO TO 203
202     EP=EXPF(AI)
        EN=EXPF(-AI)
203     CONTINUE
      CFR1=A1*(EP+EN)/2.D0
      CFI1=-A2*(EP-EN)/2.D0
      SFR1=A2*(EP+EN)/2.D0
      SFI1=A1*(EP-EN)/2.D0
      B=C1R*CBR1*CFR1-C1R*CBI1*CFI1-C1I*CBR1*CFI1-C1I*CBI1*CFR1
      B1R=B-C1R*SBR1*SFR1+C1R*SBI1*SFI1+C1I*SBR1*SFI1+C1I*SBI1*SFR1
      B1=C1I*CBR1*CFR1+C1R*CBI1*CFR1+C1R*CBR1*CFI1-C1I*CBI1*CFI1
      B1I=B1-C1I*SBR1*SFR1-C1R*SBI1*SFR1-C1R*SBR1*SFI1+C1I*SBI1*SFI1
      CBR0=1.D0-.0703125D0*ARSR/AA2+.112152D0*ARFR/AA4
      CBR0=CBR0-.572501D0*ARHR/AA6
      CBI0=+.0703125D0*ARSI/AA2-.112152D0*ARFI/AA4
      CBI0=CBI0+.572501D0*ARHI/AA6
      SBR0=-.125D0*AR/AA2+.073242D0*ARCR/AA3-.227108D0*ARPR/AA5
      SBI0=.125D0*AI/AA2-.073242D0*ARCI/AA3+.227108D0*ARPI/AA5
      A5=COSF(AR-.7853982D0)
      A6=SINF(AR-.7853982D0)
      CFR0=A5*(EP+EN)/2.D0
      CFI0=-A6*(EP-EN)/2.D0
      SFR0=A6*(EP+EN)/2.D0
      SFI0=A5*(EP-EN)/2.D0
      B0R=C1R*CBR0*CFR0-C1R*CBI0*CFI0-C1I*CBR0*CFI0-C1I*CBI0*CFR0
      B0R=B0R-C1R*SBR0*SFR0+C1R*SBI0*SFI0+C1I*SBR0*SFI0+C1I*SBI0*SFR0
      B0I=-C1I*CBI0*CFI0+C1R*CBR0*CFI0+C1R*CBI0*CFR0+C1I*CBR0*CFR0
      B0I=B0I+C1I*SBI0*SFI0-C1R*SBR0*SFI0-C1R*SBI0*SFR0-C1I*SBR0*SFR0
      B1R=-B1R
      B1I=-B1I
26    BF1R(J)=B1R
      BF1I(J)=B1I
```

```
      BFOR(J)=BOR
      BFOI(J)=BOI
C**     TYPE 999,J,B1R,B1I,BOR,BOI
      D1=BFOR(J)*BFOR(J)+BFOI(J)*BFOI(J)
      RBR(J)=(BF1R(J)*BFOR(J)+BF1I(J)*BFOI(J))/D1
30    RBI(J)=(BF1I(J)*BFOR(J)-BF1R(J)*BFOI(J))/D1
      DEL=SQRTF(3.1416D0*GZERO*.5D0)/(RP*RW)
      DELS=DEL*(2.D0-ACS)/ACS
      DELT=DEL*4.5D0*(2.D0-ACT)/ACT
      DELTD=(SQIGR+3.5D0)*(SQIGR+3.5D0)+SQIGI*SQIGI
      DELTR=DELT*(SQIGR*(SQIGR+3.5D0)+SQIGI*SQIGI)/DELTD
      DELTI=DELT*(SQIGI*(SQIGR+3.5D0)-SQIGR*SQIGI)/DELTD
      D11R=1.D0-DELS*(AR1R*RBR(1)-AR1I*RBI(1))
      D11I=-DELS*(AR1I*RBR(1)+AR1R*RBI(1))
      SD12R=AR3R*RBR(3)-AR3I*RBI(3)
      SD12I=AR3R*RBI(3)+AR3I*RBR(3)
      D12R=1.D0-(DELTR*SD12R-DELTI*SD12I)
      D12I=-DELTR*SD12I-DELTI*SD12R
      AR2AV=AR2R*AR2R+AR2I*AR2I
      SD13R=(BET1R*RBR(2)-BET1I*RBI(2))*RP/AR2AV
      SD13I=(BET1R*RBI(2)+BET1I*RBR(2))*RP/AR2AV
      D13R=SD13R*AR2R+SD13I*AR2I
      D13I=-SD13R*AR2I+SD13I*AR2R
      SD1R=D11R*D12R-D11I*D12I
      SD1I=D11R*D12I+D11I*D12R
      D1R=SD1R*D13R-SD1I*D13I
      D1I=SD1R*D13I+SD1I*D13R
      D21R=1.D0-DELS*(AR3R*RBR(3)-AR3I*RBI(3))
      D21I=-DELS*(AR3R*RBI(3)+AR3I*RBR(3))
      SD22R=AR2R*RBR(2)-AR2I*RBI(2)
      SD22I=AR2R*RBI(2)+AR2I*RBR(2)
      D22R=1.D0-(DELTR*SD22R-DELTI*SD22I)
      D22I=-DELTR*SD22I-DELTI*SD22R
      AR1AV=AR1R*AR1R+AR1I*AR1I
      SD23R=(BET2R*RBR(1)-BET2I*RBI(1))*RP/AR1AV
      SD23I=(BET2R*RBI(1)-BET2I*RBR(1))*RP/AR1AV
      D23R=SD23R*AR1R+SD23I*AR1I
      D23I=-SD23R*AR1I+SD23I*AR1R
      SD2R=D22R*D23R-D22I*D23I
      SD2I=D22R*D23I+D22I*D23R
      D2R=SD2R*D21R-SD2I*D21I
      D2I=SD2I*D21R+SD2R*D21I
      D31R=1.D0-DELS*(AR2R*RBR(2)-AR2I*RBI(2))
      D31I=-DELS*(AR2R*RBI(2)+AR2I*RBR(2))
      SD32R=AR3R*RBR(3)-AR3I*RBI(3)
      SD32I=AR3I*RBR(3)+AR3R*RBI(3)
      D32R=1.D0-(DELTR*SD32R-DELTI*SD32I)
      D32I=-DELTI*SD32R-DELTR*SD32I
      SD33R=(BET1R*RBR(1)-BET1I*RBI(1))*RP/AR1AV
      SD33I=(BET1R*RBI(1)+BET1I*RBR(1))*RP/AR1AV
      D33R=AR1R*SD33R+AR1I*SD33I
      D33I=AR1R*SD33I-AR1I*SD33R
      SD3R=D33R*D32R-D33I*D32I
      SD3I=D33R*D32I+D33I*D32R
      D3R=SD3R*D31R-SD3I*D31I
      D3I=SD3R*D31I+SD3I*D31R
      DR=D1R+D2R-D3R
      DI=D1I+D2I-D3I
      E1R=D1R
      E1I=D1I
```

```
          E21R=D11R
          E21I=D11I
          E22R=D22R
          E22I=D22I
          SE23R=(AP3R*PBR(3)-AR3I*PBI(3))/RP
          SE23I=(AR3I*PBR(3)+AP3R*PBI(3))/RP
          E23R=SE23R*BET2R-SE23I*BET2I
          E23I=SE23R*BET2I+SE23I*BET2R
          SE2R=E23R*E22R-E23I*E22I
          SE2I=E23R*E22I+E23I*E22R
          E2R=E21R*SE2R-E21I*SE2I
          E2I=E21R*SE2I+E21I*SE2R
          ER=E1R*G1SR-E1I*G1SI+E2R
          EI=E1R*G1SI+E1I*G1SR+E2I
          GSR=(ER*DR+EI*DI)/(DR*DR+DI*DI)
          GSI=(EI*DR-ER*DI)/(DR*DR+DI*DI)
          PC2PR=GSR/RFS
          PC2PI=GSI/RFS
          ARAR=SQRTF(PC2PR*PC2PR+PC2PI*PC2PI)
          PCPR=SQRTF(.5D0*(PC2PR+ARAR))
          PCPI=SQRTF(.5D0*(-PC2PR+ARAR))
          VELP=AF/PCPI
          ALFAP=PCPR
          EIV=(VELP-VEL)/VEL
          EIA=(ALFAP-ALPHA)/ALPHA
          VEL=VELP
          ALPHA=ALFAP
          PC2R=PC2PR
          PC2I=PC2PI
          IF(EIV*EIV-.0000001)41,40,40
40        GO TO 7
41        IF(EIA*EIA-.000025)43,42,42
42        GO TO 7
43        PDVP=(VELP-TV)/(DELV*100.)
          GAMAI=SRTMG/VELP
          GAMAR=ALFAP*SRTMG/AF
          RAP=(ALFAP-(TA+CA)/8.686)*(2./F*1000.)*(VELP+DELV*100.)
            ALFAP=ALFAP*8.686*100.
            ROT=ALFAP-TCA
            ADFPW=DFA*F*1000.*760./P
            ADF=ADFPW/WL
C*          ACLDF=ALFAP+ADF
C*          VAPM=DBPM-ACLDF
C*          VOAP=VAPM*100./ACLDF
C*          VAPW=VAPM*WL
            DL=(TIME-OTIME)*VELP/100.
            TDL=TDL+DL
            DABS=ALFAP*DL
            TABS=TABS+DABS
            AMPNEW=AMP*10.**(-TABS/20.)
            WRITE(8,800) TIME,TEMP,PATM,AMP,AMPNEW,TABS,TDL,ALFAP
C***
C          WRITE(3,106) RAP,FSVP,ALFAP,VELP
C          WRITE(3,107) RW,RP,GAMAR,GAMAI
CK          WRITE(3,308) F,DBPM,ACLDF,ADF
 308       FORMAT(' F=',F5.1,3X,'MS=',D9.3,3X,'CL+DIF=',D9.3,3X,'DIF=',D9.3)
C           WRITE(3,108) F,DBPM,VELP,VOAP,VAPW,FPA
          GO TO 600
99        STOP
          END
```

```
C***
C***
        SUBROUTINE VISDF(X1,X2,P,W1,W2,T,CV,VIS,DFA,OM11,OM12,OM13,
     1OM22,OM221,OM222,SM1,SM2,SM12,TS1,TS2,TS12)
        IMPLICIT REAL*8 (A-H,O-Z)
        W12=2.*W1*W2/(W1+W2)
        WM=X1*W1+X2*W2
        GM=1.+1./CV
        RR=8.3144D7
        C=(GM*RR*T/WM)**.5
        PATM=P/760.
C***
C***
C*      TYPE 12,TS12
 12     FORMAT(2X,'TS12=',F7.3)
20      FORMAT(2X,4F9.5)
        AS12=OM22/OM11
        BS12=(5.*OM12-4.*OM13)/OM11
        CS12=OM12/OM11
        SOT12=SM12*SM12*OM22
C*      TYPE 13,TS1,TS2
 13   FORMAT(2X,'TS1,TS2 :',2F8.3,/,2X,'  OMAGA(2,2)1 , OMAGA(2,2)2')
C*      TYPE 20,OM221,OM222
        SOT1=SM1*SM1*OM221
        SOT2=SM2*SM2*OM222
        V1=.000026693*(W1*T)**.5/SOT1
        V2=.000026693*(W2*T)**.5/SOT2
C       - CALCULATES VISCOSITY OF THE MIXTURE -
        V12=.000026693*(W12*T)**.5/SOT12
        XV=X1**2./V1+2*X1*X2/V12+X2**2./V2
      YV=X1**2./V1*W1/W2+X1*X2/V12*(W1+W2)/W12*V12**2./(V1*V2)
        YV=YV+X2**2./V2*W2/W1
        YV=.6*AS12*YV
      ZV=X1**2.*W1/W2+2.*X1*X2*((W1+W2)/(2.*W12)*(V12/V1+V12/V2)-1.)
        ZV=ZV+X2**2.*W2/W1
        ZV=.6*AS12*ZV
        VIS=(1+ZV)/(XV+YV)
C*      TYPE 14,T,V1,V2,VIS
14      FORMAT(3X,'T(K)',5X,'VIS(1)',5X,'VIS(2)',5X,'VIS'
     *,/,2X,F7.2,3F11.7/)
C       - CALCULATES DIFFUSION TERM -
        PD12=.002628*(T**3./W12)**.5/(SM12*SM12*OM11)
C
        RL1=.00019891*(T/W1)**.5/SOT1
        RL2=.00019891*(T/W2)**.5/SOT2
        RL12=.00019891*(T/W12)**.5/SOT12
C
        UA=4.*AS12/15.
        UB=(12.*BS12/5.+1.)/12.
        UC=(W1-W2)**2./(W1*W2)
C
        U1=UA-UB*W1/W2+UC/2.
        U2=UA-UB*W2/W1 + UC/2.
        UY=UA*(W1+W2)/(.5*W12)*RL12**2./(RL1*RL2)
        UY=UY-UB-5./(32.*AS12)*(2.4*BS12-5.)*UC
C
        XL=X1*X1/RL1 +2.*X1*X2/RL12 +X2*X2/RL2
        YL=X1*X1*U1/RL1 +2.*X1*X2*UY/RL12 +X2*X2*U2/RL2
        S1=(W1+W2)/(2.*W2)*RL12/RL1 -(W2-W1)/(2.*W1)/UA -1.
```

```
      S2=(W1+W2)*RL12/(2.*W1*RL2) -(W1-W2)/(2.*W2)/UA -1.
C
      RKT=X1*X2/(6.*RL12)*(S1*X1-S2*X2)/(XL+YL)*(6.*CS12-5.)
C     TYPE 17,C,GM,RKT
 17   FORMAT(2X,'C,GM,RKT= ',3D11.3/)
     DF=X1*X2*GM*GM*PD12/C**2.*((W1-W2)/WM +(1.-1./GM)*RKT/(X1*X2))**2.
      DFA=8.686*2.*3.1416**2./GM*DF
      AVIS=8.686*2.*3.1416**2./GM*(4./3.)*VIS*1000./(PATM*1013000.)
      ATHM=AVIS*.75*(1.+2.25/CV)*(GM-1.)/GM
      ADFPK=DFA*1000.*760./P
C     TYPE 18, AVIS,ATHM,ADFPK
 18   FORMAT(2X,'AVIS, ATHM & ADFPK(Db/WL/KhZ) :',3D11.3///)
      RETURN
      END
C***
      SUBROUTINE SSEVAL(N,U,Y,YY,SEVAL)
      IMPLICIT REAL*8 (A-H,U-Z)
      INTEGER N
      DIMENSION Y(N),YY(N)
C
      INTEGER I,J,K
      DATA I/1/
      IF(I.GE.N) I=1
      IF(U.LT.Y(I)) GO TO 10
      IF(U.LE.Y(I+1)) GO TO 30
 10   I=1
      J=N+1
 20   K=(I+J)/2
      IF(U.LT.Y(K)) J=K
      IF(U.GE.Y(K)) I=K
      IF(J.GT.I+1) GO TO 20
C
 30   DY=U-Y(I)
      DELYY=YY(I+1)-YY(I)
      DELY=Y(I+1)-Y(I)
      SEVAL=YY(I)+DY*DELYY/DELY
      RETURN
      END
C     END OF SEVAL.
     SUBROUTINE PD(W1,W2,TEMP,SM12,OM11,PD1,PD2)

C      PD CACULATES PD(PRESSURE*DIFFUSION CONSTANT) FOR BINARY
C      GAS MIXTURE
       IMPLICIT REAL*8(A-H,O-Z)
      PD1=0.002628*(TEMP**3.*(W1+W2)/(2.*W1*W2))**0.5/(SM12**2.0*OM11)
      PD2=PD1
      RETURN
       END
C     END OF PD
```

Program DAN10.DT

This program is an input data file for program RICABS.F4. It lists various action integral values for different vibrational temperatures.

0.30	2.662	2.256	1.962	2.765
0.35	2.476	2.078	1.795	2.628
0.40	2.318	1.931	1.663	2.492
0.45	2.184	1.808	1.556	2.368
0.50	2.066	1.705	1.468	2.257
0.55	1.966	1.618	1.396	2.156
0.60	1.877	1.543	1.336	2.065
0.65	1.798	1.479	1.285	1.982
0.70	1.729	1.423	1.242	1.908
0.75	1.667	1.375	1.205	1.841
0.80	1.612	1.332	1.172	1.780
0.85	1.562	1.295	1.144	1.725
0.90	1.517	1.261	1.119	1.675
0.95	1.476	1.231	1.096	1.629
1.00	1.439	1.204	1.076	1.587
1.05	1.406	1.179	1.058	1.549
1.10	1.375	1.157	1.041	1.514
1.15	1.346	1.137	1.027	1.482
1.20	1.320	1.119	1.013	1.452
1.25	1.296	1.102	1.000	1.424
1.30	1.273	1.086	.9887	1.399
1.35	1.253	1.072	.978	1.375
1.40	1.233	1.059	.9680	1.353
1.45	1.215	1.046	.9588	1.333
1.50	1.198	1.034	.9502	1.314
1.55	1.182	1.023	.9420	1.296
1.60	1.167	1.013	.9345	1.279
1.65	1.153	1.004	.9272	1.264
1.70	1.140	.9947	.9205	1.248
1.75	1.128	.9860	.9142	1.234
1.80	1.116	.9780	.9082	1.221
1.85	1.105	.9707	.9023	1.209
1.90	1.094	.9633	.8968	1.197
1.95	1.084	.9567	.8917	1.186
2.00	1.075	.9500	.8867	1.175
2.10	1.057	.9380	.8775	1.156
2.20	1.041	.9267	.8688	1.138
2.30	1.026	.9167	.8612	1.122
2.40	1.012	.9073	.8538	1.107
2.50	.9996	.8987	.8470	1.093
2.60	.9878	.8907	.8407	1.002
2.7	.9770	.8833	.8347	1.069
2.8	.9672	.8767	.8290	1.058
2.9	.9576	.8700	.8237	1.048
3.0	.9490	.8640	.8187	1.039
3.1	.9406	.8580	.8138	1.030
3.2	.9328	.8520	.8093	1.022
3.3	.9256	.8473	.8048	1.014
3.4	.9186	.8420	.8007	1.007
3.5	.9120	.8373	.7967	.9999
3.6	.9058	.8327	.7928	.9932
3.7	.8998	.8287	.7892	.9870
3.8	.8942	.8240	.7857	.9811
3.9	.8888	.8200	.7822	.9755
4.0	.8836	.8167	.7790	.9700
4.1	.8788	.8127	.7758	.9649
4.2	.8740	.8093	.7727	.9600
4.3	.8694	.8060	.7697	.9553
4.4	.8652	.8027	.7668	.9507
4.5	.8610	.7993	.7640	.9464

AD-A133 747 AMPLIFICATION OF SOUND BY GAS PHASE REACTIONS(U) 2/2
MISSISSIPPI UNIV UNIVERSITY PHYSICAL ACOUSTICS RESEARCH
GROUP H E BASS ET AL. 11 OCT 83 PARGUM-83-02
UNCLASSIFIED N00014-81-K-0691 F/G 7/4 NL

END
FILMED

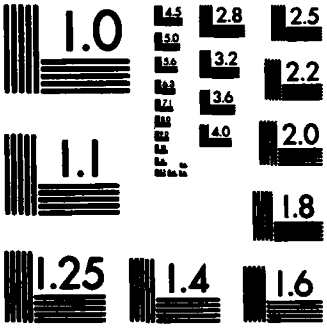

MICROCOPY RESOLUTION TEST CHART
NATIONAL BUREAU OF STANDARDS-1963-A

4.6	.8568	.7960	.7613	.9422
4.7	.8530	.7933	.7565	.9382
4.8	.8492	.7907	.7560	.9343
4.9	.8456	.7873	.7535	.9305
5.0	.8422	.7847	.7510	.9269
6.0	.8124	.7607	.7295	.8963
7.0	.7896	.7420	.7120	.8727
8.0	.7712	.7260	.6973	.8538
9.0	.7556	.7127	.6847	.8379
10.	.7424	.7013	.6735	.8242
20.	.6640	.6293	.6048	.7432
30.	.6232	.5909	.5680	.7005
40.	.5960	.5651	.5432	.6718
50.	.5756	.5459	.5248	.6504
60.	.5596	.5307	.5100	.6335
70.	.5464	.5181	.4980	.6194
80.	.5352	.5075	.4878	.6076
90.	.5256	.4984	.4790	.5973
100.	.5170	.4903	.4713	.5882

APPENDIX B

ELECTRONIC EQUIPMENT BUILT IN OUR LAB FOR cw SYSTEM

Channel no.	Circuit
0	Oscillator
1	Lamp Start
2	Filaments

Basic Principals:
--all channels are impedance-matched with non-inverting hex buffers
--channels 0 and 1 have variable delays and variable pulse widths using dual 555 timers

Channels 0 and 1

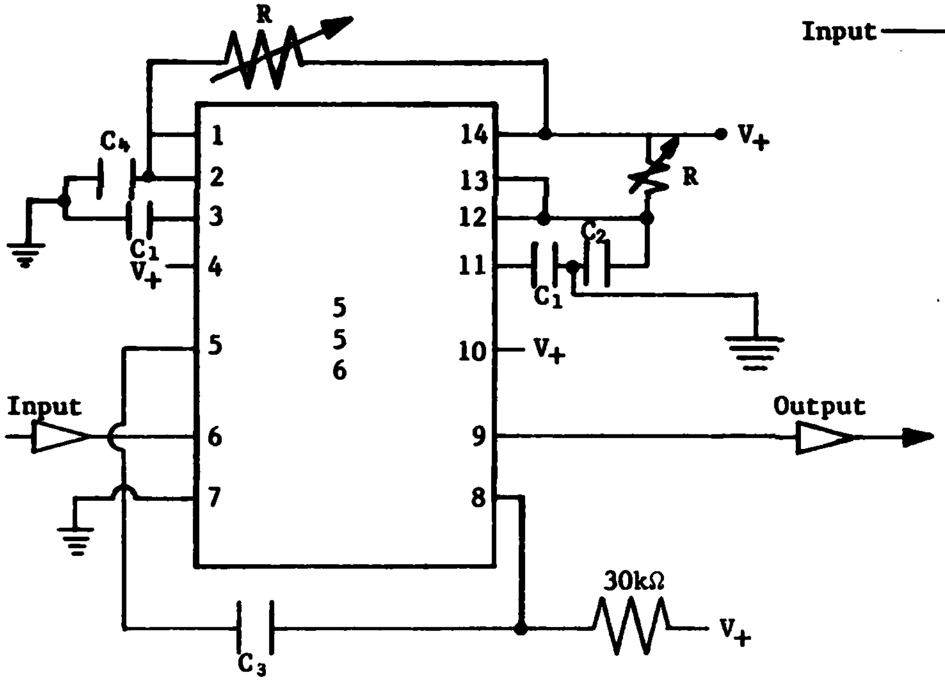

Channel 2

SYMBOLS

▷	noninverting hex buffer MC14050B
556	dual timer NE556N
V_+	5 Volts
R	0-10kΩ

CHANNELS

	0	1
C_1	.01µf	.01µf
C_2	10µf	4.7µf
C_3	.001µf	.001µf
C_4	10µf	10µf

Buffer Circuit

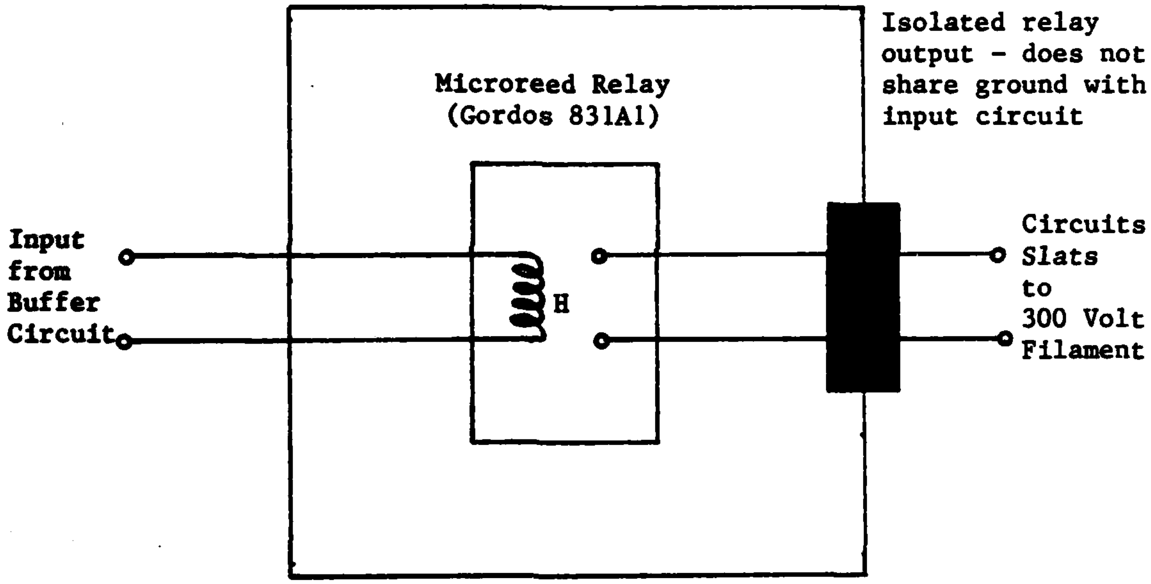

Relay Circuit for Starting Flourescent Lamps

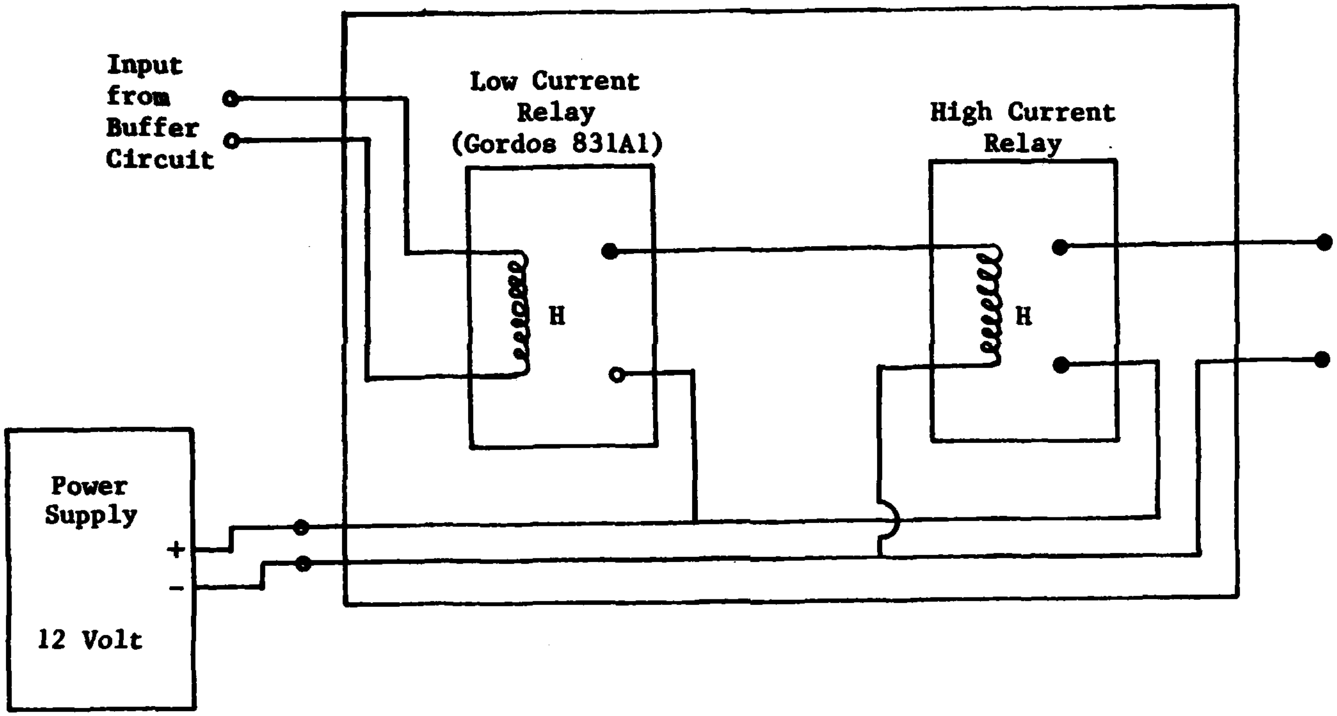

Relay Circuit for Lamp Filaments

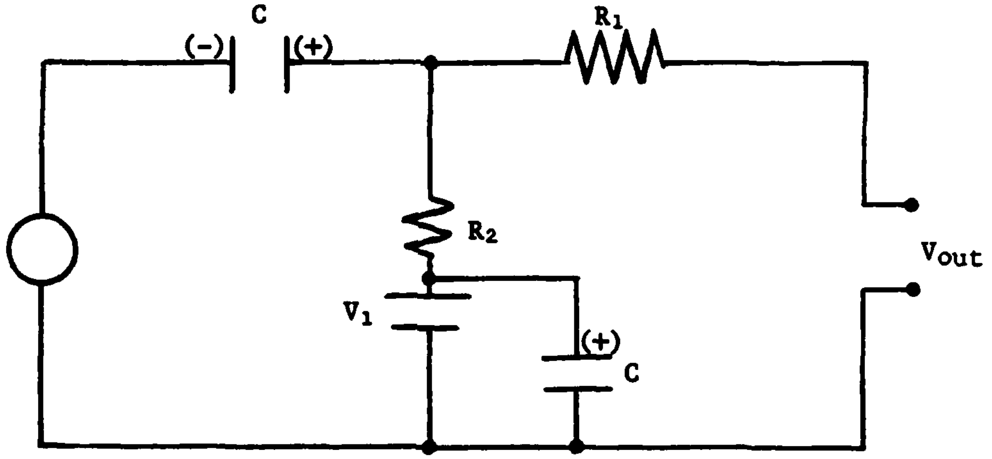

R_1 R_2	22 Ohm 1 MOhm
C	4 MFd
V_1 V_{out}	Bias Voltage Transducer Voltage

Voltage Adder for sw System Transducers

DISTRIBUTION LIST

Director Defense Advanced Research Projects Agency Attn: Technical Library 1400 Wilson Blvd. Arlington, Virginia 22209	3 copies
Office of Naval Research Physics Program Office (Code 421) 800 North Quincy Street Arlington, Virginia 22217	3 copies
Office of Naval Research Director, Technology 800 North Quincy Street Arlington, Virginia 22217	1 copy
Naval Research Laboratory Department of the Navy Attn: Technical Library Washington, D.C. 20375	3 copies
Office of the Director of Defense Research and Engineering Information Office Library Branch The Pentagon Washington, D.C. 20301	3 copies
U.S. Army Research Office Box 12211 Research Triangle Park North Carolina 27709	2 copies
Defense Technical Information Center Cameron Station Alexandria, Virginia 222314	12 copies
Director, National Bureau of Standards Attn: Technical Library Washington, D.C. 20234	1 copy
Commanding Officer Office of Naval Research Western Regional Office 1030 East Green Street Pasadena, California 91101	3 copies
Commanding Officer Office of Naval Research Eastern/Central Regional Office 666 Summer Street Boston, Massachusetts 02210	3 copies

Director 1 copy
U.S. Army Engineering Research and
Development Laboratories
Attn: Technical Documents Center
Fort Belvoir, Virginia 22060

ODDR&E Advisory Group on Electron Devices 3 copies
201 Varick Street
New York, New York 10014

Air Force Office of Scientific Research 1 copy
Department of the Air Force
Bolling AFB, D.C. 22209

Air Force Weapons Laboratory 1 copy
Technical Library
Kirtland Air Force Bas
Albuquerque, New Mexico 87117

Air Force Avionics Laboratory 1 copy
Air Force Systems Command
Technical Library
Wright-Patterson Air Force Base
Dayton, Ohio 45433

Lawrence Livermore Laboratory 1 copy
Attn: Dr. W.F. Krupke
University of California
P.O. Box 808
Livermore, California 94550

Harry Diamond Laboratories 1 copy
Technical Library
2800 Powder Mill Road
Adelphi, Maryland 20783

Naval Air Development Center 1 copy
Attn: Technical Library
Johnsville
Warminster, Pennsylvania 18974

Naval Weapons Center 1 copy
Technical Library (Code 753)
China Lake, California 93555

Naval Training Equipment Center 1 copy
Technical Library
Orlando, Florida 32813

Naval Underwater Systems Center 1 copy
Technical Center
New London, Connecticut 06320

Commandant of the Marine Corps 1 copy
Scientific Advisor (Code RD-1)
Washington, D.C. 20380

Naval Ordnance Station 1 copy
Technical Library
Indian Head, Maryland 20640

Naval Postgraduate School 1 copy
Technical Library (Code 0212)
Monterey, California 93940

Naval Missile Center 1 copy
Technical Library (Code 5632.2)
Point Mugu, California 93010

Naval Ordnance Station 1 copy
Technical Library
Louisville, Kentucky 40214

Commanding Officer 1 copy
Naval Ocean Research & Development Activity
Technical Library
NSTL Station, Mississippi 39529

Naval Explosive Ordnance Disposal Facility 1 copy
Technical Library
Indian Head, Maryland 20640

Naval Ocean Systems Center 1 copy
Technical Library
San Diego, California 92152

Naval Surface Weapons Center 1 copy
Technical Library
Silver Spring, Maryland 20910

Naval Ship Research and Development Center 1 copy
Central Library (Code L42 and L43)
Bethesda, Maryland 20084

Naval Avionics Facility 1 copy
Technical Library
Indianapolis, Indiana 46218

END

FILMED

11-83

DTIC